Non-Zero Temperature Theory for Ultra-Cold Dipolar Bose Gases

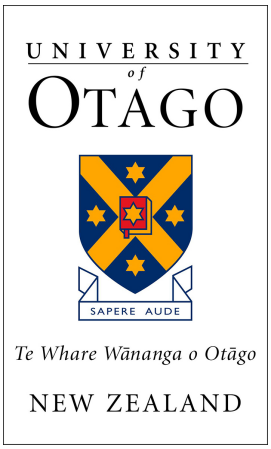

Edward Linscott

Department of Physics, University of Otago
Supervisor: Dr. P. Blair Blakie

A dissertation submitted in partial fulfillment of the requirements for the degree of BSc(Hons) in Physics, University of Otago, 2013.

Abstract

With the successful condensation of chromium, dysprosium and erbium in the past decade, physicists have begun to explore the properties of dipolar Bose gases. These gases interact via the dipole-dipole interaction, which leads to exciting and novel physics. In this dissertation I discuss the non-zero temperature theory of c-field techniques in the context of ultra-cold dipolar Bose gases in a quasi-2D geometry. I implement these methods numerically and demonstrate temperature effects on the density fluctuations and the dispersion of the system. I also identify a possible instability of dipolar systems that may prove to be important in theoretical and experimental study of these gases.

Acknowledgements

Firstly, I would like to thank my supervisor, Blair Blakie. He has been a brilliant guide throughout this year, giving me a fantastic introduction to the world of physics research. I have learned a lot from him.

I would also like to thank Russell Bisset for his collaboration. I enjoyed working alongside him and having his input and insights. Thanks also to Danny Baillie for being exceptionally generous with his time, helping me with everything from BEC theory to UNIX.

This year has been been made incredibly memorable by my ten classmates. To Rob, Lauren, Snorre, Andy, Serena, Vaughan, Malcolm, Eva, Kris, and Maddy: it has been great fun to go mad together. All the best for wherever you go next.

Thank you to my parents, who continue to be a source of endless support and encouragement.

Finally, I thank God for blessing, challenging, and teaching me throughout this year.

Contents

Introduction

Bose-Einstein condensates (BECs) have been at the forefront of physics research since their experimental realisation in 1995. BECs exhibit a range of interesting phenomena such as superfluidity, superconductivity, and coherence. The low-temperature regimes of BECs make it feasible to develop theoretical models starting with full quantum mechanical theory. These low temperatures also allow exceptional experimental control and manipulation of atoms via optical trapping.

In this dissertation I consider *dipolar* Bose gases. These species interact via the *long range* and *anisotropic* dipole-dipole interaction, which leads to completely novel behaviour unseen in other Bose gases.

Elements which exhibit strong dipolar interactions have only been condensed recently. Of these, chromium was the first to be condensed in 2005 [1], followed by dysprosium [2] and erbium [3] in 2011 and 2012 respectively. Our interest chiefly lies in gases of these atoms.

The dipole-dipole interaction has already been shown to play a crucial role in the stability and dynamics of the ^{52}Cr condensate [4, 5]. Dysprosium and erbium have only been condensed very recently, and new results from these experiments are imminent.

There is also growing interest in creating a quantum-degenerate gas of heteronuclear molecules such as KRb [6, 7]. Successfully condensing heteronuclear molecules would open the door to creating condensates with many new and interesting properties. These heteronuclear molecules possess an electric dipole far stronger than any of the magnetic dipoles possessed by a single atom. It is therefore anticipated the dipolar interactions will be very apparent in these systems, and will play an important role in their behaviour. This prompts further interest in the properties of dipolar Bose gases.[1]

Knowledge of the dipole-dipole interaction will not necessarily only apply to highly dipolar systems. In fact, the dipole-dipole interaction has been shown to play a role in systems with comparatively small magnetic dipole moments [8].

Much of the theory of Bose gases considers systems at zero temperature. However, experiments operate at temperatures that are beyond the reaches of these zero-temperature theories. For that reason, we are interested in non-zero temperature theory.

[1] Admittedly, the most success thus far has been made with fermionic species, but there are also groups working with bosons.

In this dissertation, I study dipolar Bose gases using the non-zero temperature theory of "c-field techniques". These techniques provide an approximate description of the ultra-cold Bose gas for temperatures approaching the critical temperature. Popular non-zero techniques such as Hartree-Fock-Bogoliubov-Popov encounter difficulties with dipolar systems, and our c-field approach provides an alternative.

Before considering non-zero temperatures and c-field techniques, I will discuss the zero-tempearture theory of dipolar Bose gases. I do this in Chapter 1. I then discuss the numerical implementation of two c-field techniques. I consider the *projected Gross-Pitaevskii equation* in Chapter 2, and then the *stochastic projected Gross-Pitaevskii equation* in Chapter 3. Using these two techniques I identify an instability of the dipolar system, and explore the effect of temperature on its density fluctuations. As I conclude, I will outline possible avenues of further research.

Chapter 1

Zero Temperature Theory

In this chapter I discuss the standard theoretical treatment of dilute and dipolar Bose gases at *zero* temperature. This will serve as a starting point for the non-zero temperature approaches I'll introduce in later chapters.

1.1 The Dipole-Dipole Interaction

Let us begin by considering the properties of the dipolar interaction.

Some atoms possess a large magnetic moment, arising from their total angular momentum J. This magnetic moment means the atoms interact via the long range and anisotropic dipole-dipole interaction.[1]

The potential energy of two dipoles with dipole moments $\mathbf{d}_1$ and $\mathbf{d}_2$ separated by $\mathbf{x} = \mathbf{x}_1 - \mathbf{x}_2$ is given by

$$V_d(\mathbf{x}) = \frac{1}{|\mathbf{x}|^3}\left(\mathbf{d}_1 \cdot \mathbf{d}_2 - 3(\hat{\mathbf{x}} \cdot \mathbf{d}_1)(\hat{\mathbf{x}} \cdot \mathbf{d}_2)\right) \tag{1.1}$$

In this dissertation, I restricted my attention to identical dipoles with dipole moments aligned along the z direction. If they each have dipole moment $\mathbf{d}$, the dipole potential takes the form

$$V_d(\mathbf{x}) = \frac{d^2}{|\mathbf{x}|^3}\left(1 - 3\cos^2\theta\right) \tag{1.2}$$

where $\cos\theta = \hat{\mathbf{x}} \cdot \hat{\mathbf{d}}$. The basic properties of this potential are discussed in Figure 1.1.

[1] Molecules can also interact via the dipole-dipole interaction. But for the case of heteronuclear molecules, these interactions would be due to the molecules' *electric* dipole moment. Nevertheless, the dipole-dipole interaction here is unchanged from the magnetic case - so while I will focus on atomic gases, the case of molecular gases is equivalent.

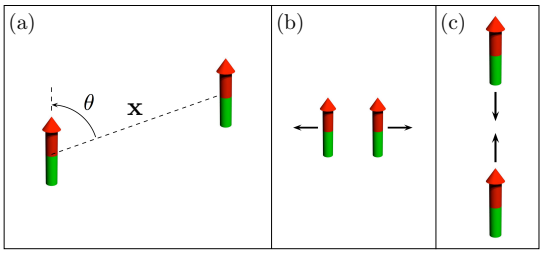

Figure 1.1: The basics of the dipole-dipole interaction (a) The interaction between two dipoles is proportional to $1/\mathbf{x}^3$, and angle-dependent (b) For two side-by-side dipoles, the interaction is repulsive (c) For head-to-tail dipoles, the interaction is attractive. In essence, they behave much like "bar-magnets". Figure adapted from [9]

It is this anisotropic and long range character of the interactions that leads to the completely novel physics we witness in dipolar systems.

We can see from Equation 1.2 that the interaction strength is proportional to the square of the dipole moment d. There are a number of other parameters that are used to describe this interaction strength, and I will pause to introduce these now.

The scattering properties of contact interactions can be described by the s-wave scattering length a. The equivalent length scale for *dipolar* interactions is defined as $a_{dd} \coloneqq md^2/3\hbar^2$, where m is the mass of the atom and d its dipole moment. We then define the interaction coupling g as related to a scattering length a by

$$g \coloneqq \frac{4\pi a\hbar^2}{m} \tag{1.3}$$

As we will see, the interaction couplings g (contact) and g_{dd} (dipole-dipole) will be the defining parameters of our dipolar systems. The values of these parameters for a number of key atomic and molecular species are summarised in Table 1.1.

Table 1.1: Dipole moments and scattering lengths of selected atoms and molecules

Species	Dipole Moment	a_{dd} (a_0)
^{87}Rb	1 μ_B	0.71
^{52}Cr	6 μ_B	15.4
^{168}Er	7 μ_B	67.6
^{164}Dy	10 μ_B	134
^{41}K^{87}Rb	0.6 Debye	3940

1.2 Quasi-Two-Dimensional Geometry

Experimentally, a Bose gas must be confined by some sort of trap. And because of the anisotropic nature of the dipole-dipole interaction, the physics of a dipolar system is hugely dependent on the trap geometry.

We will consider a quasi-two-dimensional (quasi-2D) trap geometry. This geometry has a tight level of confinement in z direction, but no confinement in the x-y plane. More explicitly, we have an external trap potential of $U(\mathbf{x}) = \frac{1}{2}m\omega_z^2 z^2$. We define the corresponding harmonic oscillator length as $l_z \coloneqq \sqrt{\hbar/m\omega_z}$.

At low (yet experimentally realisable) temperatures, the energy of oscillations in the z-direction is significantly larger than $k_\mathrm{B}T$. Consequently, the gas in the direction of tight confinement undergoes zero-point oscillations, and we can separate out the z-component of the wave function as the ground-state wavefunction of a harmonic potential;

$$\chi(z) = \frac{1}{{l_z}^{1/2}\pi^{1/4}}\exp\left(-\frac{z^2}{2{l_z}^2}\right) \tag{1.4}$$

since the lowest z-vibrational mode is usually occupied. This leaves us with an essentially 2D wavefunction,

$$\Psi(\mathbf{x}) = \chi(z)\psi(\boldsymbol{\rho}) \tag{1.5}$$

where $\psi(\boldsymbol{\rho})$ is the wavefunction in the x-y plane and $\boldsymbol{\rho} = (x, y)$. This is known as the single mode approximation, and is valid where interaction energies are small compared to $\hbar\omega_z$".

For example, the group in Stuttgart who condensed chromium uses a trap with a length of $l_z \approx 1300\ a_0$ (where a_0 is the Bohr radius) [10]. So for temperatures less than 200 nK, we would lie in this limit.

However, it is important to note that the problem we are faced with is not wholly two-dimensional. The dipoles typically interact at length scales smaller than the trap size. (To return to the example of the experiment in Stuttgart, chromium's dipole length is 15 a_0, many times smaller than their trap length of $l_z \approx 1300\ a_0$.) This means that the dipoles are not forced to lie in a plane side-by-side; some may possibly be head-to-tail.

This has important ramifications for how we treat g, the interaction coupling parameter that dictates the strength of dipolar interactions. The parameter g we introduced earlier applies to a three-dimensional system, and as we go from three dimensions to quasi-2D, we must modify it. Petrov et al. [11] showed that for a quasi-2D Bose gas at

ultra-cold but non-zero temperatures, the interaction coupling takes the form

$$g_{\mathrm{q2D}} = \frac{2\sqrt{2\pi}\hbar^2}{m}\frac{1}{l_z/a - 1/\sqrt{2\pi}\ln(\pi k^2 {l_z}^2)} \tag{1.6}$$

Consider the limit $a \ll l_z$. This means that the length scales of the trap in the z-direction are much longer than the length scales of the interactions. In this limit, g takes the form

$$g_{\mathrm{q2D}} = \frac{g}{\sqrt{2\pi}l_z} \tag{1.7}$$

which, aside from a constant, is simply the three dimensional result. Therefore, we retain *three*-dimensional scattering theory, despite reducing the wave function to two dimensions.

This quasi-2D geometry is, in some ways, a simplistic limiting case. Of course, in an experiment one cannot have an infinite plane of atoms — they must be somehow confined in the x-y directions, too. And to date, experiments with dipolar gases have not quite reached quasi-2D regimes. Nevertheless, the quasi-2D problem is still worthwhile considering. Quasi-2D simulations reproduce the same results qualitatively as much more complicated simulations. For a fuller discussion on the applicability of the quasi-2D problem, see Appendix A.1.

1.3 The Gross-Pitaevskii Equation

Having considered the interactions and geometry of our system, we will now develop the governing equations for an ultracold dilute Bose gas. Since the system is dilute, we only need to concern ourselves with two-body interactions. The many body Hamiltonian is therefore

$$\hat{H} = \int d\mathbf{x}\ \hat{\Psi}^\dagger(\mathbf{x},t)\hat{H}^{(1)}\hat{\Psi}(\mathbf{x},t) + \frac{1}{2}\int d\mathbf{x}\int d\mathbf{x}'\ \hat{\Psi}^\dagger(\mathbf{x},t)\hat{\Psi}^\dagger(\mathbf{x}',t)V(\mathbf{x}-\mathbf{x}')\hat{\Psi}(\mathbf{x}',t)\hat{\Psi}(\mathbf{x},t) \tag{1.8}$$

where $V(\mathbf{x}-\mathbf{x}')$ is some (as of yet unspecified) interaction potential that will account for contact and dipole-dipole interactions, and $\hat{H}^{(1)}$ is the single particle Hamiltonian

$$\hat{H}^{(1)} = -\frac{\hbar^2\nabla^2}{2m} + U(\mathbf{x}) \tag{1.9}$$

where m is the mass of a single particle and $U(\mathbf{x})$ is the external trapping potential.

The evolution of the field operator $\hat{\Psi}(\mathbf{x})$ is governed by the equation

$$\begin{aligned} i\hbar\frac{\partial}{\partial t}\hat{\Psi}(\mathbf{x},t) &= [\hat{\Psi}(\mathbf{x},t),\hat{H}] \\ &= \left(-\frac{\hbar^2\nabla^2}{2m}+U(\mathbf{x})+\int d\mathbf{x}'\ \hat{\Psi}^\dagger(\mathbf{x}',t)V(\mathbf{x}-\mathbf{x}')\hat{\Psi}(\mathbf{x}',t)\right)\hat{\Psi}(\mathbf{x},t) \end{aligned} \tag{1.10}$$

At $T=0$, the gas will be fully condensed, and one can replace the operator $\hat{\Psi}(\mathbf{x},t)$ with the classical field $\Psi(\mathbf{x},t)$.[2] With the correct steps taken, one can obtain the time-dependent *Gross-Pitaevskii equation* (GPE)

$$i\hbar\frac{\partial}{\partial t}\Psi(\mathbf{x},t)=\left(-\frac{\hbar^2\nabla^2}{2m}+U(\mathbf{x})+\int d\mathbf{x}'\ \Psi^*(\mathbf{x}',t)V(\mathbf{x}-\mathbf{x}')\Psi(\mathbf{x}',t)\right)\Psi(\mathbf{x},t) \tag{1.11}$$

but now $V(\mathbf{x}-\mathbf{x}')$ is a low energy effective interaction potential. The energy functional for this system is given by

$$\begin{aligned} E[\psi(\mathbf{x})] = \int d\mathbf{x}\Bigg(&\frac{\hbar^2}{2m}|\nabla\Psi(\mathbf{x})|^2+U(\mathbf{x})|\Psi(\mathbf{x})|^2 \\ &+\frac{1}{2}\int d\mathbf{x}'\ \Psi^*(\mathbf{x})\psi^*(\mathbf{x}')V(\mathbf{x}-\mathbf{x}')\Psi(\mathbf{x}')\psi(\mathbf{x})\Bigg) \end{aligned} \tag{1.12}$$

Note that if the condensate wave function is given by

$$\Psi(\mathbf{x},t)=\Psi(\mathbf{x})\exp\left(-\frac{i\mu t}{\hbar}\right) \tag{1.13}$$

where we define the chemical potential $\mu=\frac{\partial E}{\partial N}$ then the GPE reduces to the *time-independent* GPE

$$\left(-\frac{\hbar^2\nabla^2}{2m}+U(\mathbf{x})+\int d\mathbf{x}'\ \Psi^*(\mathbf{x}')V(\mathbf{x}-\mathbf{x}')\Psi(\mathbf{x}')\right)\Psi(\mathbf{x})=\mu\Psi(\mathbf{x}) \tag{1.14}$$

This equation was derived independently by Gross [13] and Pitaevskii [14] in 1961. It is the main theoretical tool for considering dilute Bose gases.

[2]The interaction potential must be treated carefully when this substitution is made; see [12].

The GPE in Quasi-2D

In the case of a quasi-2D gas we can use the decomposition $\Psi(\mathbf{x}) = \chi(z)\psi(\boldsymbol{\rho}, t)$ (equation 1.5) to remove the z-dependence of our problem. For the time dependent GPE, making this substitution gives

$$\begin{aligned} &i\hbar\frac{\partial}{\partial t}\psi(\boldsymbol{\rho}, t)\chi(z) \\ &\quad = \left(-\frac{\hbar^2\nabla^2}{2m} + \frac{1}{2}m\omega_z^2 z^2 + \int d\mathbf{x}'\ \psi^*(\boldsymbol{\rho}', t)\chi^*(z')V(\mathbf{x}-\mathbf{x}')\psi(\boldsymbol{\rho}', t)\chi(z')\right)\psi(\boldsymbol{\rho}, t)\chi(z) \end{aligned} \tag{1.15}$$

where $\boldsymbol{\rho} = (x, y)$, and we have used the quasi-2D trap potential $U(\mathbf{x}) = \frac{1}{2}m\omega_z^2 z^2$. If we then multiply by $\chi^*(z)$ and integrate over z we obtain

$$\begin{aligned} i\hbar\frac{\partial}{\partial t}\psi(\boldsymbol{\rho}, t) = \Bigg(&-\frac{\hbar^2\nabla_{\boldsymbol{\rho}}^2}{2m} + \frac{1}{2}\hbar\omega_z \\ &+ \int dz \int d\mathbf{x}'\ \chi^*(z)\chi^*(z')\Psi^*(\boldsymbol{\rho}', t)V(\mathbf{x}-\mathbf{x}')\Psi(\boldsymbol{\rho}', t)\chi(z')\chi(z)\Bigg)\psi(\boldsymbol{\rho}, t) \end{aligned} \tag{1.16}$$

Since we know $\chi(z)$ explicitly, carrying out this integration removes any z-dependence from the problem. We can also ignore the constant factor of $\frac{1}{2}\hbar\omega_z$, as it only leads to an inconsequential energy shift.

1.4 Interaction Potentials in Quasi-2D

We now look to incorporate both contact and dipolar interactions into the Gross-Pitaevskii equation we have just established.

Our objective is to evaluate the integral

$$\int dz \int d\mathbf{x}'\ \chi^*(z)\chi^*(z')\psi^*(\boldsymbol{\rho}')V(\mathbf{x}-\mathbf{x}')\psi(\boldsymbol{\rho}')\chi(z')\chi(z) \tag{1.17}$$

as this is the form in which the interaction potential appears in the quasi-2D time dependent GPE (equation 1.16), and elsewhere.

Case 1: Contact Interactions

For the contact component we use the pseudopotential $V_c(\mathbf{x}-\mathbf{x}') = g\delta(\mathbf{x}-\mathbf{x}')$. It is important to note that atomic contact interactions are far more complicated than this "bowling-ball"-like potential indicates. However for the case of dilute systems like ours, and at the low collision energies relevant at ultra-cold temperatures, the actual form of the two-body potential is unimportant, and this pseudopotential is adequate for describing the interactions. Using this pseudopotential, equation 1.17 becomes

$$g\int dz\int d\mathbf{x}'\ \psi^*(\mathbf{x}')\delta(\mathbf{x}-\mathbf{x}')\psi(\mathbf{x}') = g|\psi(\boldsymbol{\rho})|^2\int dz\ |\chi(z)|^4 = \frac{g}{\sqrt{2\pi}l_z}|\psi(\boldsymbol{\rho})|^2 \quad (1.18)$$

This coefficient can be recognised as the quasi-2D interaction coupling g_{q2D}.

Case 2: Dipole-Dipole Interactions

Incorporating the dipolar potential is more involved than the contact case, and will not be shown here, but is instead included in Appendix A.2. The key results of the derivation are as follows.

Firstly, it is advantageous to transform the effective interaction potential into k-space. There, it takes the form

$$\tilde{V}_{\mathrm{d}}(\mathbf{k}_\rho) = \frac{g_{dd}}{\sqrt{2\pi}l_z}F\left(\frac{\mathbf{k}_\rho l_z}{\sqrt{2}}\right) \qquad \text{where} \qquad F(\mathbf{q}) = 2-3\sqrt{\pi}qe^{q^2}\mathrm{erfc}(\mathbf{q}) \quad (1.19)$$

where $\mathrm{erfc}(q)$ is the complementary error function. Then the integral 1.17 can be evaluated via the convolution theorem, and is found to be

$$\int dz\int d\mathbf{x}'\ \psi^*(\mathbf{x}')V_d(\mathbf{x}-\mathbf{x}')\psi(\mathbf{x}') = \mathcal{F}^{-1}[\tilde{V}_{\mathrm{d}}(\mathbf{k}_{\boldsymbol{\rho}})n(\mathbf{k}_{\boldsymbol{\rho}})] =: \Phi_D(\boldsymbol{\rho}) \quad (1.20)$$

where $\mathcal{F}$ is the fourier transform, and $n(\mathbf{k}_{\boldsymbol{\rho}}) = \mathcal{F}(|\psi(\boldsymbol{\rho})|)^2$ is the momentum-space density.

The Total Interaction Potential

Before incorporating all of these results into the GPE, it is worthwhile pausing for a moment to consider the behaviour of the effective total potential (contact plus dipole)

$$\tilde{V}(\mathbf{k}_{\boldsymbol{\rho}}) = \tilde{V}_c(\mathbf{k}_{\boldsymbol{\rho}}) + \tilde{V}_d(\mathbf{k}_{\boldsymbol{\rho}}) = \frac{1}{\sqrt{2\pi}l_z}\left(g + g_{dd}F\left(\frac{k_{\boldsymbol{\rho}}l_z}{\sqrt{2}}\right)\right) \quad (1.21)$$

Note that $\tilde{V}(\mathbf{k}_{\boldsymbol{\rho}})$ is actually dependent on the magnitude, but not the direction of $\mathbf{k}_{\boldsymbol{\rho}}$

This function is plotted in Figure 1.2 for a range of g and g_{dd}.

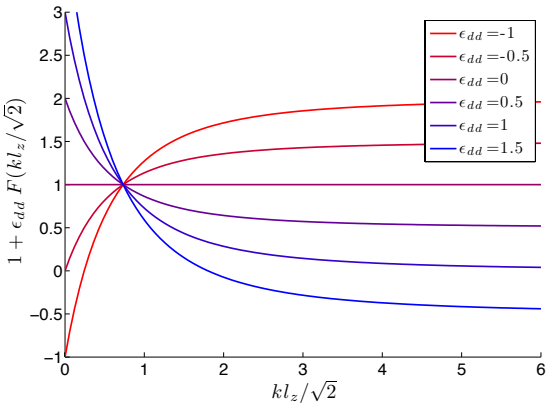

Figure 1.2: The behaviour of the total effective potential of a Bose gas with contact and dipolar interactions in quasi-2D. ϵ_{dd} is defined as g_{dd}/g. Note that if the function drops below 0 the interaction has become attractive.

$F(q)$ has the limiting behaviour

$$\lim_{q\to 0} F(q) = 2 \tag{1.22}$$

$$\lim_{q\to \infty} F(q) = -1 \tag{1.23}$$

Namely, the dipolar interaction is repulsive at low k-values, but attractive at high k-values. This is interpreted in Figure 1.3

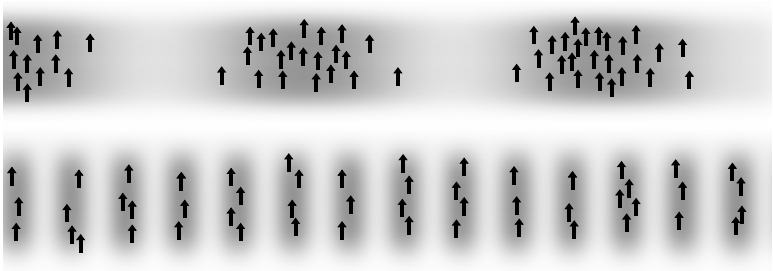

Figure 1.3: An intuitive way to consider the limiting behaviour of $\tilde{V}(\mathbf{k})$. Excitations with low k-values (corresponding to long wavelengths) leave the dipoles largely side-by-side, where they are repulsive, so $\tilde{V}(\mathbf{k})$ is positive. On the other hand, high k-value excitations (short wavelengths) arrange the dipoles end-to-end, where they are attractive, so $\tilde{V}(\mathbf{k})$ is negative.

We are finally ready to incorporate both contact and dipolar interactions into the time independent GPE. Combining our calculations for both cases, the interaction term becomes

$$\int dz \int d\mathbf{x}' \; \chi^*(z)\chi^*(z')\psi^*(\boldsymbol{\rho}',t)V(\mathbf{x}-\mathbf{x}')\psi(\boldsymbol{\rho}',t)\chi(z')\chi(z) = g_{\mathrm{q2D}}|\psi(\boldsymbol{\rho},t)|^2 + \Phi_D(\boldsymbol{\rho},t) \tag{1.24}$$

So for a Bose gas with contact and dipolar interactions, the time independent GPE becomes

$$i\hbar\frac{\partial}{\partial t}\psi(\boldsymbol{\rho},t) = \left\{-\frac{\hbar^2\nabla^2}{2m} + g_{\mathrm{q2D}}|\psi(\boldsymbol{\rho},t)|^2 + \Phi_D(\boldsymbol{\rho},t)\right\}\psi(\boldsymbol{\rho},t) \tag{1.25}$$

While this only holds at strictly zero temperature, it will serve as our starting point for developing non-zero temperature theory.

From now we will be exclusively considering this two dimensional problem, and I will simply write "$\mathbf{x}$" instead of "$\boldsymbol{\rho}$".

1.5 Excitations and the Bogoliubov Approximation

We will now consider the elementary excitations of a Bose gas at zero temperature. To do this, a standard perturbative approach is to assume that the gas is almost exclusively in the condensate, and then linearise any excitations about the condensate.

An equivalent procedure[3] is to diagonalise the system's Hamiltonian via the substitution

$$\hat{a}_0, \;\; \hat{a}_0^\dagger \rightarrow \sqrt{N_0} \tag{1.26}$$

This amounts to assuming the gas is almost fully condensed, since if $N_0 \gg 1$ it follows that

$$\hat{a}_0|N_0,0,0,...\rangle \approx \sqrt{N_0}|N_0,0,0,...\rangle \qquad \hat{a}_0^\dagger|N_0,0,0,...\rangle \approx \sqrt{N_0}|N_0,0,0,...\rangle \tag{1.27}$$

This approach was first suggested by Bogoliubov [15], and is known as the Bogoliubov approximation. A full derivation of the diagonalsiation procedure can be found in Appendix A.4. Here, I will give an outline of the procedure and discuss the results. We begin with the Hamiltonian of equation 1.8:

$$\hat{H} = \int d\mathbf{x} \; \hat{\Psi}^\dagger(\mathbf{x})\hat{H}^{(1)}\hat{\Psi}(\mathbf{x}) + \frac{1}{2}\int d\mathbf{x}\int d\mathbf{x}' \; \hat{\Psi}^\dagger(\mathbf{x})\hat{\Psi}^\dagger(\mathbf{x}')V(\mathbf{x}-\mathbf{x}')\hat{\Psi}(\mathbf{x}')\hat{\Psi}(\mathbf{x}) \tag{1.28}$$

[3] We demonstrate this equivalence in Appendix A.5.

We then adopt this Hamiltonian to a quasi-2D geometry in a similar manner as we did for the time dependent GPE in Section 1.3. Having done this, we are left with a field operator $\hat{\psi}(\mathbf{x})$ that is two dimensional and unconfined. To handle this "infinite" field, we restrict our attention to a square cell of edge length L, and adopt the plane wave basis

$$\hat{\psi}(\mathbf{x}) = \sum_{\mathbf{k}} \frac{1}{L} e^{i\mathbf{k}\cdot\mathbf{x}} \hat{a}_{\mathbf{k}} \tag{1.29}$$

Using this basis, the Hamiltonian can be recast as

$$\hat{H} = \sum_{\mathbf{k}} \frac{\hbar^2 k^2}{2m} \hat{a}^\dagger_{\mathbf{k}} \hat{a}_{\mathbf{k}} + \frac{1}{2L^2} \sum_{\mathbf{k}_1,\mathbf{k}_2,\mathbf{q}} \tilde{V}(\mathbf{q}) \hat{a}^\dagger_{\mathbf{k}_1+\mathbf{q}} \hat{a}^\dagger_{\mathbf{k}_2-\mathbf{q}} \hat{a}_{\mathbf{k}_1} \hat{a}_{\mathbf{k}_2} \tag{1.30}$$

By employing the Bogoliubov approximation $\hat{a}_0,\ \hat{a}^\dagger_0 \to \sqrt{N_0}$, the Hamiltonian separates into terms proportional to ${N_0}^2$, ${N_0}^{3/2}$, N_0, and so on. It can then be diagonalised up to the order of N_0.

In diagonalising the Hamiltonian, we introduce the quasiparticle operators $\hat{\alpha}_{\mathbf{k}}$ and $\hat{\alpha}^\dagger_{\mathbf{k}}$ as follows

$$\begin{array}{rcl} \hat{a}_{\mathbf{k}} = & u_k \hat{\alpha}_{\mathbf{k}} - v_k \hat{\alpha}^\dagger_{-\mathbf{k}} \\ \hat{a}^\dagger_{-\mathbf{k}} = & u_k \hat{\alpha}^\dagger_{-\mathbf{k}} - v_k \hat{\alpha}_{\mathbf{k}} \end{array} \quad \Longrightarrow \quad \begin{array}{rcl} \hat{\alpha}_{\mathbf{k}} = & u_k \hat{a}_{\mathbf{k}} + v_k \hat{a}^\dagger_{-\mathbf{k}} \\ \hat{\alpha}^\dagger_{-\mathbf{k}} = & u_k \hat{a}^\dagger_{-\mathbf{k}} + v_k \hat{a}_{\mathbf{k}} \end{array} \tag{1.31}$$

where u_k and v_k are some suitably chosen coefficients.

These quasiparticle operators allow us to rewrite the Hamiltonian of equation 1.28 as

$$\hat{H} \approx \frac{1}{2} n_{2D} N \tilde{V}(\mathbf{0}) + \frac{1}{2} \sum_{\mathbf{k}\neq 0} \left(E_k - \epsilon^0_k - n\tilde{V}(\mathbf{k}) \right) + \frac{1}{2} \sum_{\mathbf{k}\neq 0} E_k \left(\hat{\alpha}^\dagger_{\mathbf{k}} \hat{\alpha}_{\mathbf{k}} + \hat{\alpha}^\dagger_{-\mathbf{k}} \hat{\alpha}_{-\mathbf{k}} \right) \tag{1.32}$$

where

$$\epsilon^0_k = \frac{\hbar^2 k^2}{2m} \quad \text{and} \quad E_k = \sqrt{\epsilon^0_k (\epsilon^0_k + 2n\tilde{V}(\mathbf{k}))} \tag{1.33}$$

n is the two-dimensional density of the gas, and $\tilde{V}(\mathbf{k})$ is the interaction potential that we discussed in Section 1.4.

The Bogoliubov Dispersion

It is important to notice that having diagonalised the Hamiltonian, the quantity E_k is the quasiparticle dispersion relation of our system. It is of much interest, and it is worthwhile exploring its possible behaviour. To reiterate, it is of the form

$$E_k = \sqrt{\epsilon_k^0(\epsilon_k^0 + 2n\tilde{V}(\mathbf{k}))} \tag{1.34}$$

Recall that $\tilde{V}(\mathbf{k})$ is a function of g and g_{dd}, and is given by

$$\tilde{V}(\mathbf{k}) = \frac{1}{\sqrt{2\pi}l_z}\left(g + g_{dd}F\left(\frac{kl_z}{\sqrt{2}}\right)\right) \tag{1.35}$$

Therefore, the shape of the dispersion relation will be dependent on these two parameters g and g_{dd}, and the two-dimensional density of the gas n. Changing these parameters will give us different dispersion relations.

Different atomic species possess different values of g and g_{dd}. But we are not simply restricted to considering the pairs of $\{g, g_{dd}\}$ belonging to each element in turn.

For Bose gases, the s-wave scattering length (and therefore g) can be tuned as desired using Fano-Feshbach resonance [16, 17]. Furthermore, it is proposed that the dipole strength g_{dd} can also be tuned by rapidly rotating the dipole orientation [18].

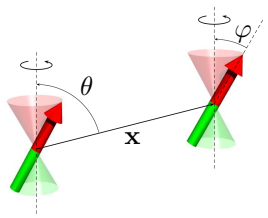

Figure 1.4: Tuning the strength of dipolar interactions. If the dipoles are rotated sufficiently quickly via an external magnetic field, the time-averaged dipole strength can be weakened, or even made negative, by changing the dipoles' offset angle φ. We should admit that rotating dipoles like this would very hard to implement experimentally. By tilting the dipoles relative to the z-direction (but not rotating them) we can weaken the dipolar interaction, but this does introduce anisotropy into the system and alters the character of the dipole-dipole interaction. While not discussed here, this remains a very interesting problem. Figure taken from [9]

Given that we can tune these parameters, we can explore a range of "domains", as illustrated in Figure 1.5.

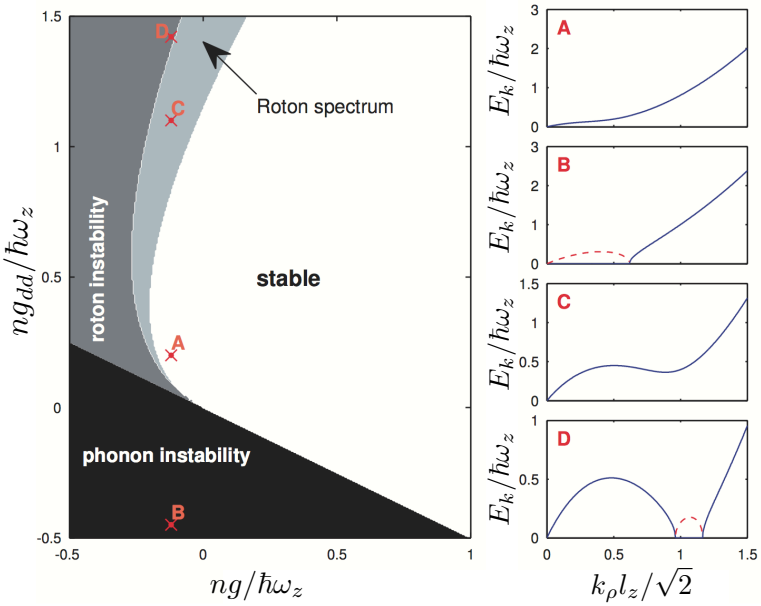

Figure 1.5: Stability phase diagram and some associated dispersion relations for a quasi-2D dipolar Bose gas. In the white and light grey regions, the gas is dynamically stable. In the white region, the dispersion is monotonically increasing, with a linear dispersion at low k (phonons) and quadratic at high k (free particle). In the light grey region dipolar interactions lead to a local minimum, or "roton". In the black region, low k excitations are unstable. (This is represented by the dotted red line, indicating an imaginary E_k). In the dark grey region, the dipolar interactions are so strong that the roton minimum becomes imaginary, and hence the system becomes unstable. Figure adapted from [19].

Rotons

The idea of rotons first appeared in the study of superfluidity in ^{4}He. Following its discovery 1938, there was great interest in attempting to explain liquid helium's unusual non-dissipative behaviour. Landau (among others) suggested that superfluidity arose because a fraction of the system became BEC-like [20]. He therefore proposed a two-fluid model to describe liquid ^{4}He, with one fluid corresponding to the superfluid component, and the other to the non-superfluid component. He also suggested that within the non-superfluid component there existed localised quantised vortices, or "rotons", and that these rotons experience quadratic dispersion.

Indeed, the dispersion of ^{4}He has a roton feature, as shown in Figure 1.6.

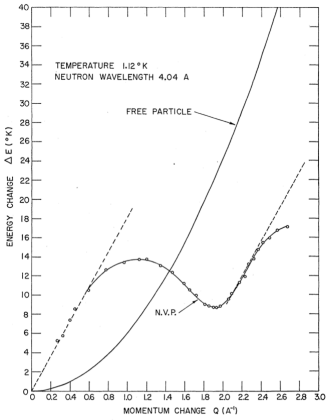

Figure 1.6: Dispersion curve for ^{4}He. Note the linear phonon dispersion at small momenta, and the roton at $\sim 2\text{Å}^{-1}$. Figure taken from [21].

It must be noted that the relation between the roton feature and local vorticity within the fluid remains unclear. It is not even certain if the roton feature is at all associated with vorticity. Nozières proposed an alternative viewpoint [22]. He suggested the roton minimum in ^{4}He is instead a precursor to crystallisation, eloquently describing the roton as "the ghost of the Bragg spot". In other words, it is the system "threatening" to become crystalline.

Filinov *et al.* considered dipolar bosonic molecules in a pure-2D geometry (where all of the dipoles are held tightly side-by-side in a plane). With these exceptionally strong dipoles and very tight confinement, a crystalline phase appeared that seemed associated with the onset of roton instability. So perhaps in this case, Nozières' proposal may have some truth to it.

In our case of a quasi-2D Bose gas, what exactly we mean physically by "rotons" is even less clear. We must content ourselves with our fairly abstract idea of them as elementary excitations at wave numbers corresponding to a local minimum in the dispersion.

Although we may not know what exactly rotons are, it is this roton minimum that leads to the novel physics of dipolar gases.

Chapter 2

The Projected Gross-Pitaevskii Equation

In the previous chapter we considered a dipolar Bose gas at zero temperature. At zero temperature an almost pure BEC forms, which is well described by the GPE, and we were able to consider elementary excitations via Bogoliubov theory.

We now turn our attention to higher temperature cases where the GPE alone provides an inadequate description of the system. Experiments routinely operate at temperatures well beyond the reaches of the Bogoliubov approximation, and we would like to be able to consider these regimes theoretically.

Faced with this problem, we turn to a different description of Bose gases that does not force us to make such strong assumptions, and yet for which the problem remains tractable. These techniques are known generically as *c-field* methods. Implementation of these methods is one of the primary achievements of this dissertation.

2.1 C-field Methods and the PGPE

Bogoliubov theory was derived by assuming that we have appreciable occupation of the ground state. C-field methods recognise that at nonzero temperatures this will not only be true of the ground state. Indeed, many other modes will also have an occupation much greater than one quantum. These modes therefore behave somewhat like a classical field - hence the name "c-field methods".

Generically, c-field methods divide the system into two distinct regions:

- the **c-field region (C-region)** contains the condensate and all other highly degenerate modes. This region is evolved using field equations of a similar form to the GPE, but with a few key modifications.
- the **incoherent region (I-region)** contains the modes are sparsely occupied. The modes in this region have a weak influence on the dynamics of the C-region.

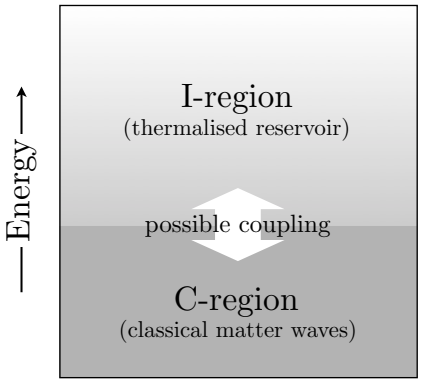

Figure 2.1: Schematic view of the system. The low energy modes of the C-region behave like classical matter waves, whereas the I-region can be considered as a thermalised reservoir.

Formally, we suppose the occupation of a plane wave mode $N_{\mathbf{k}}$ is much greater than $[\hat{a}_{\mathbf{k}}, \hat{a}^{\dagger}_{\mathbf{k}}] = 1$ for not just the ground state, but for some larger set of modes. This defines our C-region. We can then define the c-field operator

$$\hat{\psi}(\mathbf{x}) \coloneqq \mathcal{P}\hat{\Psi}(\mathbf{x}) = \sum_{\mathbf{k}\in C} \hat{a}_{\mathbf{k}}\varphi_{\mathbf{k}}(\mathbf{x}) \tag{2.1}$$

where we choose $\{\varphi_{\mathbf{k}}(\mathbf{x})\}$ to be the plane-wave basis,[1]

$$\varphi_{\mathbf{k}}(\mathbf{x}) = \frac{1}{L} e^{i\mathbf{k}\cdot\mathbf{x}} \tag{2.2}$$

Given that all C-region modes are appreciably occupied, quantum fluctuations are negligible and we may set $\hat{\psi}(\mathbf{x}) \to \psi(\mathbf{x})$. This is done by making the replacement $\hat{a}_{\mathbf{k}},\ \hat{a}^{\dagger}_{\mathbf{k}} \to c_{\mathbf{k}}$, in which case

$$\psi(\mathbf{x}) = \sum_{\mathbf{k}\in C} c_{\mathbf{k}}\varphi_{\mathbf{k}}(\mathbf{x}) \tag{2.3}$$

It is also useful to define a second projector $\mathcal{Q} = 1 - \mathcal{P}$. This allows us to consider the Bose field operator in the I-region, $\mathcal{Q}\hat{\Psi}(\mathbf{x}) = \hat{\eta}(\mathbf{x})$. In this region, the average occupation of the modes is less than one, so quantum fluctuations are important. For this reason we do not make any substitutions for $\hat{a}_{\mathbf{k}}$ or $\hat{a}^{\dagger}_{\mathbf{k}}$ as we did in the C-region.

[1] Recall that to handle the "infinite" x-y plane of our quasi-2D system, we restrict our attention a square cell of edge length L. Our choice of $\{\varphi_{\mathbf{k}}(\mathbf{x})\}$ therefore gives an orthonormal basis.

As introduced in Section 1.3, the equation of motion for the full Bose operator is

$$i\hbar\frac{\partial}{\partial t}\hat{\Psi}(\mathbf{x},t)=\left(-\frac{\hbar^2\nabla^2}{2m}+\int d\mathbf{x}'\ \hat{\Psi}^\dagger(\mathbf{x}',t)V(\mathbf{x}-\mathbf{x}')\hat{\Psi}(\mathbf{x}',t)\right)\hat{\Psi}(\mathbf{x},t) \tag{2.4}$$

We can now separate $\hat{\Psi}(\mathbf{x})$ into $\psi(\mathbf{x})$ and $\hat{\eta}(\mathbf{x})$ in this equation of motion. Having done this, we project into the C-region to look at the dynamics of $\psi(\mathbf{x})$. The resulting equation one would obtain is the *finite temperature GPE* (FTGPE). It is a complicated and lengthy equation, and so is not included here.[2]

The FTGPE describes the full dynamics of the system $\psi(\mathbf{x})$ and its coupling to a thermal bath $\hat{\eta}(\mathbf{x})$, accounting for all of the coupling between the C- and I-regions. In the equation, there appear five interaction terms. These are pictorially illustrated in Figure 2.2.

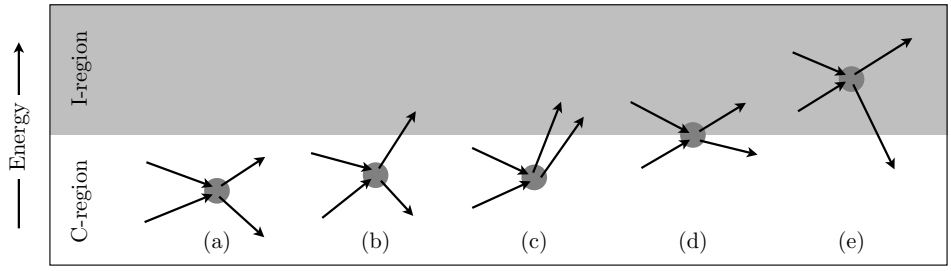

Figure 2.2: Processes accounted for in the FTGPE formalism: (a) interactions within the C-region, with both particles remaining in the C-region; (b) growth/loss processes arising from interactions within the C-region, leading to particle and energy exchange between the regions (c) the so-called "anomalous" term, which cannot conserve energy and therefore cannot describe real processes in and of itself (d) scattering processes, leading to energy but not particle exchange between the C- and I-regions (e) growth/loss processes arising from interactions within the I-region, leading to particle and energy exchange between the regions

Importantly, the *only* assumption we made in the derivation of the FTGPE was the condition that the modes in the C-region were highly occupied. It should therefore be valid whenever this condition is satisfied: we haven't yet had to make many restricting assumptions.

However, the FTGPE is hardly any simpler than the original equation of motion. After all, all we have done is separate the field operator into two parts and replaced

[2]See [23] for a complete derivation of the FTGPE for a gas with contact interactions only. The dipolar case is analogous, if a little more complicated.

some operators. Furthermore, if we were to attempt to solve it, we would also need an equation of motion for the I-region dynamics. To make the problem tractable, we must therefore decide to ignore some of the interaction processes. The key difference between different c-field methods lies in this decision.

In the remainder of this dissertation, I will describe two of these c-field methods, how I implemented them numerically, and the behaviour I observed in subsequent simulations.

The first c-field method I will consider is the *projected GPE* (PGPE). This treatment considers near-equilibrium behaviour. In these regimes, we assert that all interactions between the C- and I-regions (terms b to e) are sufficiently weak that we can ignore them. Under this assumption, the FTGPE reduces to

$$i\hbar\frac{\partial}{\partial t}\psi(\mathbf{x}) = \left(-\frac{\hbar^2\nabla^2}{2m} + g_{\mathrm{q2D}}|\psi(\mathbf{x})|^2 + \Phi_D(\mathbf{x})\right)\psi(\mathbf{x}) \tag{2.5}$$

This is the PGPE. It is simply the GPE extended to cover the C-region. Since there are no interactions between the C- and I-regions, the PGPE is a *microcanonical* system: the energy and particle number of the C-region is *conserved*.

2.2 Implementing the PGPE

To explore what the PGPE predicts about the dynamical and equilibrium properties of Bose gases, we must turn to numerical simulations. We are now in a position to do this.

I had access to pre-existing MATLAB® code that implemented evolution according to the PGPE for a quasi-2D Bose gas with contact interactions only.

This code solves the PGPE using a 4-5 Runge-Kutta algorithm with an adaptive step size. The C-region is chosen to be all plane-wave modes below a predetermined cutoff k value. This allows us to implement the projection operator in Fourier space easily.

I modified the preexisting MATLAB® code to incorporate dipolar effects, by introducing the additional term $\Phi_D(\mathbf{x})$ that accounts for dipolar interactions, which was defined as

$$\Phi_D(\mathbf{x}) \coloneqq \mathcal{F}^{-1}[\tilde{V}_{\mathrm{d}}(\mathbf{k}_{\boldsymbol{\rho}})n(\mathbf{k}_{\boldsymbol{\rho}})] \tag{2.6}$$

where $\mathcal{F}$ is the fourier transform, $n(\mathbf{k}_{\boldsymbol{\rho}}) = \mathcal{F}|(\psi(\boldsymbol{\rho}))|^2$ is the momentum-space density,

and

$$F(\mathbf{q}) = 2 - 3\sqrt{\pi} q e^{q^2} \mathrm{erfc}(\mathbf{q}) \tag{2.7}$$

Care needs to be taken when numerically evaluating the complementary error function for large q. We make use of an asymptotic expansion to overcome this problem (see Appendix A.3).

Dimensionless Variables

It is useful to choose dimensionless units for computational purposes. Let us consider the full time-independent GPE with contact and dipolar interactions (as found in Section 1.4):

$$\mu\psi(\mathbf{x}) = -\frac{\hbar^2\nabla^2}{2m}\psi(\mathbf{x}) + \left(g_{\mathrm{q2D}}|\psi(\mathbf{x})|^2 + \Phi_{dd}(\mathbf{x})\right)\psi(\mathbf{x}) \tag{2.8}$$

The units for the energy, length, and time scales we choose are

$$\hbar\omega_z, \qquad l_z = \sqrt{\hbar/m\omega_z}, \qquad \tau = 1/\omega_z, \qquad T_0 = \frac{\hbar\omega_z}{k_B} \tag{2.9}$$

It is then helpful to make the coupling interactions dimensionless by defining

$$\tilde{g} = \frac{mg}{\sqrt{2\pi} l_z \hbar^2} \tag{2.10}$$

in which case we obtain the dimensionless form of the GPE

$$\tilde{\mu}\tilde{\psi}(\tilde{\mathbf{x}}) = -\frac{\tilde{\nabla}^2}{2}\tilde{\psi}(\tilde{\mathbf{x}}) + \left(\tilde{g}|\tilde{\psi}(\tilde{\mathbf{x}})|^2 + \tilde{\Phi}_D(\tilde{\mathbf{x}})\right)\tilde{\psi}(\tilde{\mathbf{x}}) \tag{2.11}$$

where all the quantities used are now with respect to our dimensionless variables.[3] These are the units that I adopted for numerical computations, and are used in all the figures. But unless otherwise noted, I do not adopt them for equations in the body of this dissertation.

[3]Note that Φ_D contains an interaction coupling constant g_{dd}, which must be is scaled in the same manner as g.

2.3 Algorithm Validation

Having developed this code, it was critical to ensure it was properly evaluating the PGPE. To do this, we conducted an extensive array of tests.

Firstly, as the wavefunction evolves according to the PGPE, its energy must be conserved and it must stay normalised. In our dimensionless units, the energy and number functionals are given in turn by

$$\tilde{E}[\tilde{\psi}(\tilde{\mathbf{x}})] = \frac{1}{2}\int d\tilde{\mathbf{k}}\; k^2|\tilde{\phi}(\tilde{\mathbf{k}})|^2 + \frac{1}{2}\int d\tilde{\mathbf{x}}\left(\tilde{g}|\tilde{\psi}(\tilde{\mathbf{x}})|^4 + \tilde{\Phi}_D(\tilde{\mathbf{x}})|\tilde{\psi}(\tilde{\mathbf{x}})|^2\right) \tag{2.12}$$

$$\tilde{N}[\tilde{\psi}(\tilde{\mathbf{x}})] = \int d\tilde{\mathbf{x}}\; |\tilde{\psi}(\tilde{\mathbf{x}})|^2 \tag{2.13}$$

where $\tilde{\phi}(\tilde{\mathbf{k}}) = \mathcal{F}(\tilde{\psi}(\tilde{\mathbf{x}}))$. We found for typical[4] simulations that both energy and particle number were conserved up to a factor of approximately 10^{-11}.

Of course, these are simple checks but we would be gravely concerned if these quantities changed with time. A less trivial test involves the chemical potential. If we have pure and uniform condensate with density $\sqrt{n}$, then the time evolution of the wavefunction is given by

$$\psi(\mathbf{x}, t) = \psi_0(\mathbf{x})e^{-i\mu t/\hbar} = \sqrt{n}e^{-i\mu t/\hbar} \tag{2.14}$$

This can be calculated using the GPE. Furthermore, the chemical potential can be explicitly calculated using the time-independent GPE and the $k \to 0$ limit of $\tilde{V}(\mathbf{k})$ (equations 1.14 and 1.22). We find that

$$\tilde{\mu} = \tilde{n}(\tilde{g} + 2\tilde{g}_{dd}) \tag{2.15}$$

This was compared to the phase evolution ascribed to the condensate by the PGPE code, and these two values were found to match (up to machine precision).

[4] 10,000-step simulations with a Runge-Kutta error tolerance of 10^{-4}

Single Quasiparticle Excitations

Here we describe a further test where we show that linearised excitations of our system reproduce the expected Bogoliubov quasiparticles.

Recall that at low temperatures, our system acts like a set of non-interacting quasiparticles, as defined by

$$\hat{\alpha}_{\mathbf{k}} = u_{\mathbf{k}}\hat{a}_{\mathbf{k}} + v_{\mathbf{k}}\hat{a}^{\dagger}_{-\mathbf{k}} \tag{2.16}$$

and these quasiparticles have a dispersion relation given by

$$E_k = \sqrt{\epsilon^0_k(\epsilon^0_k + 2n\tilde{V}(\mathbf{k}))} \tag{2.17}$$

Inspired by the form of the quasiparticle operator, we consider a wavefunction of the form

$$\psi(\mathbf{x}) = \psi_0(\mathbf{x}) + \frac{\lambda}{L}\left\{u_q e^{i\mathbf{q}\cdot\mathbf{x}} - v_q e^{-i\mathbf{q}\cdot\mathbf{x}}\right\} \tag{2.18}$$

for some small constant λ. This wavefunction corresponds to a condensate with an excitation in a single quasiparticle mode with wave vector $\mathbf{q}$. If we substitute this wavefunction into the time-dependent Gross-Pitaevskii (equation 1.11), we can derive its evolution.[5] We find to first order in λ that

$$\psi(\mathbf{x},t) = e^{-i\mu t/\hbar}\left(\psi_0(\mathbf{x}) + \frac{\lambda}{L}\left[u_q e^{i(\mathbf{q}\cdot\mathbf{x}-\omega_q t)} - v_q e^{-i(\mathbf{q}\cdot\mathbf{x}-\omega_q t)}\right]\right) \tag{2.19}$$

where $\omega_q = E_q/\hbar$ is the corresponding frequency of the quasiparticle excitation as given by equation 2.17.

To make this comparison, we proceeded as follows

1. We construct an initial wavefunction as per equation 2.18, for some chosen $\mathbf{q}$
2. The wavefunction was then evolved using the PGPE code, and we measured the phase $\mp\theta_q$ with which the $\pm\mathbf{q}$ *plane* wave modes evolved. As this phase changed linearly with time we could determine ω_q via $\theta_q = \omega_q t$
3. This was then repeated for an array of different $\mathbf{q}$. In this manner, we amassed a set of data points $\{(\mathbf{q}, \omega_q)\}$

These data points ought to match the Bogoliubov dispersion of equation 2.19. The results of these simulations are shown in Figure 2.3.

[5] This derivation is contained in Appendix A.5

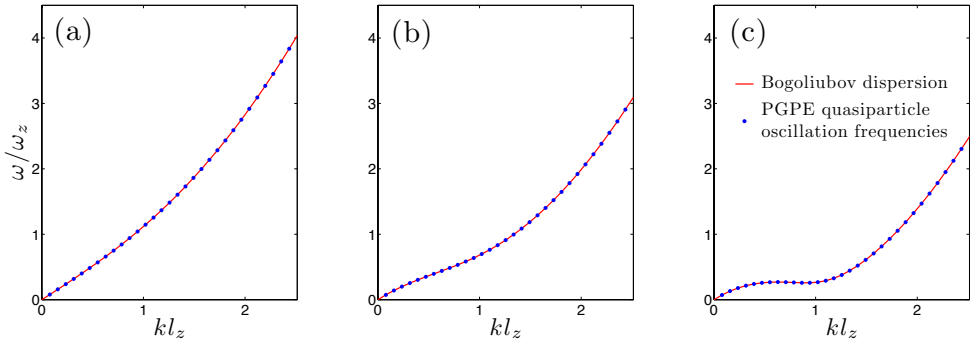

Figure 2.3: Quasiparticle phase evolution for three systems: (a) has only contact interactions ($g = 0.25$), (b) is weakly dipolar ($g = 0.05$, $g_{dd} = 0.10$) and (c) is strongly dipolar ($g = -0.05$, $g_{dd} = 0.15$). Each blue point shows a data point $(\mathbf{q}, \omega_q)$ — the oscillation frequency ω_q of a single quasiparticle with a given wave vector $\mathbf{q}$, as found using a PGPE simulation. The dispersion relation E_q obtained via a Bogoliubov approach is shown in red.

The quasiparticle phase evolution clearly matches the Bogoliubov dispersion relation, and these results gave us confidence that the dipolar PGPE code was functioning correctly.

Getting our code to pass these tests took a considerable amount of time and was instrumental in removing a number of bugs.

2.4 A Near-Equilibrium Wavefunction

A condensate with a small amplitude quasiparticle excitation lies within the linearised region. Our interest lies in far more energetic systems where the quasiparticles are highly occupied and can interact.

Previous studies have shown that systems evolving according to the PGPE can thermalise [24]. By this, I mean that these systems tend towards and settle at some equilibrium state. As mentioned already, the energy and particle number of our system is conserved, so the equilibrium state should be determined by these macroscopic constraints.

When we began to investigate the evolution of some contrived wavefunctions, it quickly became apparent that wavefunctions evolving according to the PGPE are slow to equilibrate. To minimise computation time, it was worthwhile putting some thought into what initial wavefunction we chose to evolve. The three initial wavefunctions we considered are shown in Figure 2.4

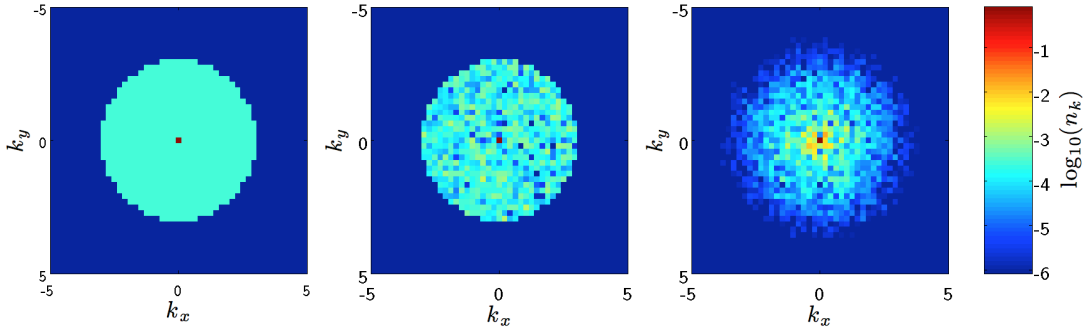

Figure 2.4: Density plots of three choices for the initial wave function: (left) the **"top hat"** has uniform occupation of all modes below some energy cut-off. What is not visible from this figure is that each mode is also given a random phase; (centre) the **"noisy top hat"** is the same as the previous case, but now the occupation of the modes below the cut-off are normally distributed; (right) finally, we can make an educated guess for a **near-equilibrium wave function**, as discussed below.

The "top-hat" wavefunction was used in [24] to directly study thermalisation. It this study, it was shown to equilibrate after ∼50,000 time steps. In their case, this "top hat" was a sensible choice for an initial wavefunction, as it makes thermalisation clearly visible. Our interest, however, lies in the equilibrium properties of the gas, so we would like to avoid having to wait that long before the system thermalises. With that in mind, we will now construct an improved initial wavefunction.

In Appendix A.5 we show that the excitations of a ground state can be written as

$$\hat{\psi}(\mathbf{x}) = \psi_0(\mathbf{x}) + \hat{\varphi}(\mathbf{x}) = \psi_0(\mathbf{x}) + \sum_{j\neq 0}\left[u_j(\mathbf{x})\hat{\alpha}_j - v_j^*(\mathbf{x})\hat{\alpha}_j^\dagger\right] \tag{2.20}$$

where $u_k(\mathbf{x})$ and $v_k(\mathbf{x})$ are of the form

$$\begin{aligned} u_k(\mathbf{x}) &= u_k \frac{e^{i\mathbf{k}\cdot\mathbf{x}}}{L} \\ v_k(\mathbf{x}) &= v_k \frac{e^{i\mathbf{k}\cdot\mathbf{x}}}{L} \end{aligned} \tag{2.21}$$

and u_k and v_k are the coefficients associated with the quasiparticles, that are defined in equation A.27.

We would expect that each of the quasiparticle modes would be approximately occupied according to the Bose-Einstein distribution.

$$\langle \hat{\alpha}_{\mathbf{k}}^{\dagger} \hat{\alpha}_{\mathbf{k}} \rangle \approx \frac{1}{e^{\beta \epsilon_k} - 1} = N_{BE} \tag{2.22}$$

where ϵ_k is the energy of the mode k, as calculated by the Bogoliubov dispersion, and $\beta = 1/k_B T$. Of course, the Bose-Einstein distribution only holds for the case of non-interacting modes. Our quasiparticle modes will be interacting, but equation 2.22 can serve as an approximation. We also know that we have the ensemble averages

$$\langle \hat{\alpha}_{\mathbf{k}} \rangle = \langle \hat{\alpha}_{\mathbf{k}} \hat{\alpha}_{\mathbf{k}} \rangle = \langle \hat{\alpha}_{\mathbf{k}}^{\dagger} \hat{\alpha}_{\mathbf{k}}^{\dagger} \rangle = 0 \tag{2.23}$$

Therefore, we generate a set of numbers $\{\alpha_{\mathbf{k}}\}$ by

$$\alpha_{\mathbf{k}} = \sqrt{\frac{N_{BE}}{2}} (x_{\mathbb{R}} + i x_{\mathbb{I}}) \tag{2.24}$$

where $x_{\mathbb{R}}$ and $x_{\mathbb{I}}$ are from a set of normally distributed random numbers. This choice means that $\alpha_{\mathbf{k}}$ mimics the behaviour of the quasiparticle operators; namely

$$\overline{|\alpha_{\mathbf{k}}|^2} = \frac{1}{e^{\beta \epsilon_k} - 1} \qquad \text{and} \qquad \overline{\alpha_{\mathbf{k}}} = \overline{\alpha_{\mathbf{k}}{}^2} = \overline{(\alpha_{\mathbf{k}}^*)^2} = 0 \tag{2.25}$$

We can then use these random numbers $\alpha_{\mathbf{k}}$ to generate the "near-equilibrium" wave function

$$\psi(\mathbf{x}) = \psi_0(\mathbf{x}) + \sum_{\mathbf{k}} \left(u_k \alpha_{\mathbf{k}} \frac{e^{i\mathbf{k}\cdot\mathbf{x}}}{L} - v_k \alpha_{\mathbf{k}}^* \frac{e^{-i\mathbf{k}\cdot\mathbf{x}}}{L} \right) \tag{2.26}$$

This wavefunction should be near to equilibrium, so it will serve as a better starting point for our simulations than the highly contrived "top hats". Of course, in its construction we have ignored interactions between each quasiparticle mode, which is an oversimplification. We should not be surprised if even this wavefunction takes some time to equilibrate.

2.5 System Behaviour

Now, we will examine the behaviour of this near-equilibrium wave function when it is evolved according to the PGPE.

We will be considering cases with different interaction strengths. Unless otherwise stated, we will be consider the three cases from Figure 2.3. I will refer to these as simply the "contact only", "weakly dipolar", and "strongly dipolar" cases respectively. All simulations had a particle number of $N = 25600$, a box length $L = 80$, and a cut-off energy $\epsilon_{cut} = 5$.

Firstly, let us examine the effects of introducing dipolar interactions to the system.

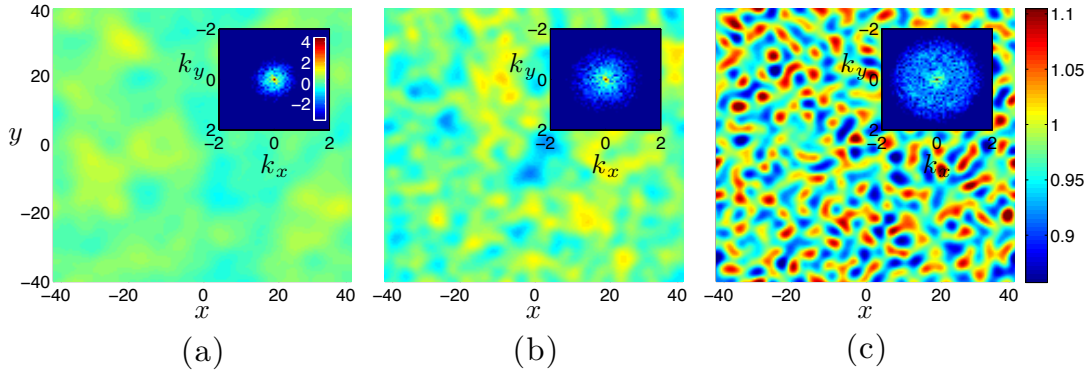

Figure 2.5: The system after time 100τ in the three cases (a) contact interactions only (b) weakly dipolar (c) strongly dipolar/rotonic, corresponding to the cases explored in Figure 2.3. The main figure shows position space occupation $N(\mathbf{x}) = |\psi(\mathbf{x})|^2 d\mathbf{x}$, and the inset shows the k-space profile $\log_{10} N(\mathbf{k}) = \log_{10}\left(|\mathcal{F}(\psi(\mathbf{x}))|^2 d\mathbf{k}\right)$. The near-equilibrium wavefunction with $T = 0.1$ was chosen as the initial wavefunction.

The key difference of note is the "halo" in the k-space density of the strongly dipolar case (c). This system had a shallow roton minimum at $k \approx 1$, which matches the k at which this halo appears. As expected, these low-energy rotonic modes become readily occupied.

This halo manifests itself in the corresponding position space density, where we see larger fluctuations. Furthermore, these fluctuations seem to be of a regular size. To investigate this further, consider what happens when we stay rotonic, but tune the parameters g and g_{dd} to move the roton feature to different k values (Figure 2.6).

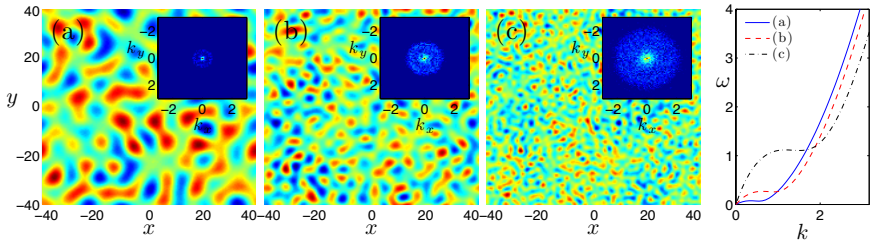

Figure 2.6: The density of the system with different roton minima at time $\tau = 100$. Again, the main image shows the position space density, and the inset the k-space density. The corresponding dispersion relations are shown on the right. T was chosen in each case to make the roton modes weakly occupied ($T = 0.01$, 0.1, and 0.25 respectively).

It can be seen that the size of the real space fluctuations approximately correspond to the rotonic wavelength.

We now consider what happens when we increase the energy of the initial wavefunction. After all, we introduced the PGPE as a tool for going to temperatures beyond the validity of Bogoliubov theory.

In practice we increase the energy of our system by tuning the T parameter used in constructing the initial wave function. To reiterate what was shown in the previous section, we choose an initial wavefunction

$$\psi(\mathbf{x}) = \psi_0(\mathbf{x}) + \sum_{\mathbf{k}} \left(u_k \alpha_{\mathbf{k}} e^{i\mathbf{k}\cdot\mathbf{x}} - v_k \alpha^*_{\mathbf{k}} e^{-i\mathbf{k}\cdot\mathbf{x}} \right) \tag{2.27}$$

where $\{\alpha_{\mathbf{k}}\}$ was a set of numbers generated by

$$\alpha_{\mathbf{k}} = \sqrt{\frac{1}{2} \frac{1}{e^{\epsilon_k / k_B T} - 1}} (x_{\mathbb{R}} + i x_{\mathbb{I}}) \tag{2.28}$$

It is critical to keep in mind that T is *not* the temperature of our system. When we constructed this initial wavefunction at some "temperature" T, we were considering non-interacting modes. Now, we have introduced interactions, so it is no longer clear what the actual temperature of the system is.[6]

Since system energy and particle number are conserved, we implicitly specify these parameters in our choice of the parameter T.[7]

[6] If we desire to determine the actual temperature of the system, we must infer it indirectly. Doing this is not entirely straightforward (see [24]).

[7] With all these caveats, T may seem a poorly chosen parameter now. However, in later chapters it will give us something to compare to.

That note aside, let us consider the effect of increasing the energy of a rotonic system.

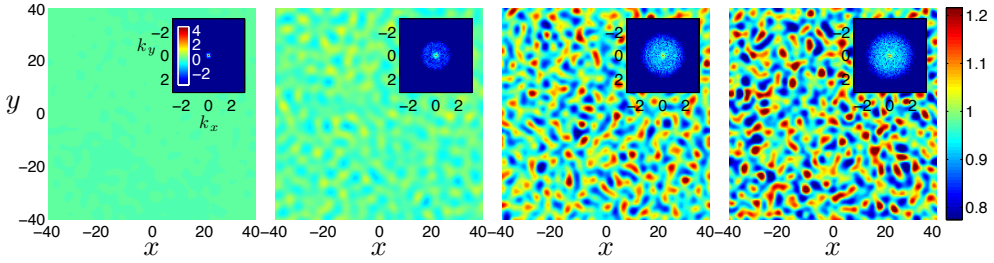

Figure 2.7: The position and k-space densities for the strongly dipolar system at time $\tau = 100$ with the parameter $T = 0.01$, 0.05, 0.1, and 0.125.

This behaves as expected: at low temperatures, the gas is almost exclusively in the condensate. As temperature increases, the higher k modes become more occupied as, the gas fluctuates more, and the roton "halo" becomes clearly visible.

The energies we've considered here are still comparatively low. The condensate fraction for these cases have been about 0.99, and we are interested in the behaviour of systems with higher energies. However, when we tried to consider these more energetic systems, something dramatic happened.

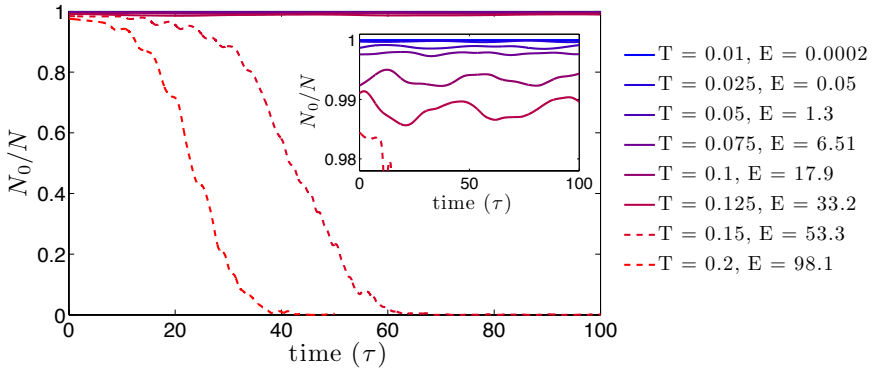

Figure 2.8: The condensate fraction as a function of time for the strongly dipolar/rotonic case, for different values of T (and hence different values of E). These simulations had $N = 25600$, $L = 80$, and $\epsilon_{cut} = 5$

For high values of the parameter T, the condensate fraction drops suddenly. Looking at the lower temperature cases, there is no apparent reason why these higher temperature cases would suddenly display such dramatically different behaviour.

To clarify what is going on here, let us look at the position-space density during one of these collapses.

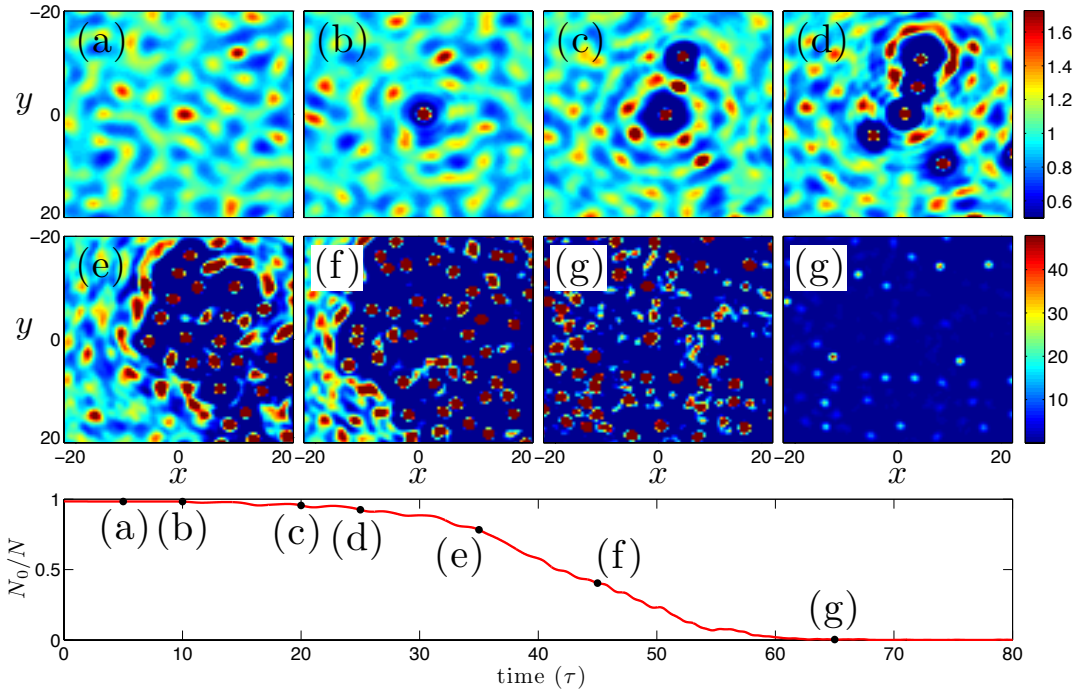

Figure 2.9: Position space density as the strongly dipolar system collapses for $T = 0.15$. The lowermost plot displays again the condensate fraction, but now we additionally look at the position space density at seven different times (a to g) during collapse. For the first seven tiles, the bounds on the color range are fixed, as given by the upper colour bar. (For this reason, the final images seem to be purely maroon and blue, because the density greatly exceeds the bounds.) In the eighth and final tile I replot case g with new bounds.

An area of large local density, or a "pimple", forms. By pulling nearby gas into itself, the pimple grows in density (but not in size). And as it grows, neighbouring pimples start to form, until this blight has spread throughout all of the system.

But while the first seven tiles give a good impression as to how this spreading occurs, perhaps the eighth tile is the most illuminating as to what is going on: the gas seems to be collapsing into local density spikes. But it is only natural to ask, is what we are observing here physical?

Soliton-Like Phenomena

It occurred to us that what we are witnessing could be the formation of solitons.

A soliton is a non-dissipative, self-reinforcing solitary wave. The concept of a "wave of translation" was first noted by John Scott Russell in 1844 [25], who wrote

> *"...I was observing the motion of a boat which was rapidly drawn along a narrow channel by a pair of horses, when the boat suddenly stopped — not so the mass of water in the channel which it had put in motion; it ... rolled forward with great velocity, assuming the form of a large solitary elevation, a rounded, smooth and well-defined heap of water, which continued its course along the channel apparently without change of form or diminution of speed..."*

These observations of a single, stable wave seemed at odds with the hydrodynamic theory of Newton and Bernoulli, and this disagreement was only resolved in the 1870s by Boussinesq and Rayleigh [26, 27].

The nonlinearity of the physics of BECs lead to such local and stable waves. Solitons have been experimentally observed in BECs (see [28], for example). Furthermore, they have been predicted to form in *dipolar* Bose gases in the case where the dipolar interaction g_{dd} has been tuned to become weak and *negative* [29, 30]. Santos *et al.* reported that if a phonon instability[8] arose, a transient gas of solitons could form and thus the system may avoid collapse.

In contrast, we observed these soliton-like features in regions nearing *roton* (not phonon) collapse, since we consider positive values for g_{dd}.

We used a variational ansatz to assess the stability of our features. We were unable to locate any stable solutions (which is why I've been referring to the features as "soliton-like").

We therefore expect that these features are unphysical. Let us reconsider what happens as the system collapses. During collapse, the system begins to occupy progressively higher energy modes. However, our system is restricted to the C-region; all of the modes our system can access are below some cut-off energy. Once the highest energy modes have become occupied, the cut-off energy will stabilise the system, resulting in the formation of "pimples". In this scenario, our separation of the system into the C- and I-regions is invalid.

[8] That is to say, if the system crosses from the white to the black region in Figure 1.5

2.6 Leaving the PGPE

While these "pimple" features are unphysical, that does not mean that the collapse itself is unphysical too. The existence of this instability is significant in and of itself. Identifying this instability is one of the notable achievements of this chapter.

The reader may be justifiably concerned that these collapses occur at such low energies. At these low energies, one would think that Bogoliubov theory would hold — and Bogoliubov theory does not predict any instabilities. However, Boudjemâa and Shlyapnikov proposed earlier this year that satisfying the conditions necessary for Bogoliubov theory to apply is much harder in rotonic systems than in the contact case [31]. This may explain why Bogoliubov apparently fails at such low temperatures.

Our interest in stability aside, these "pimples" were an obstacle. They first appeared when we attempted to consider rotonic gases, thereby preventing us from studying this regime. The interesting dynamics of dipolar gases will be the strongest here, so we want to somehow reach these regimes, if possible.

Furthermore, the limited ability of the PGPE to thermalise was proving to be a hindrance. When we compared the evolution of "top hat" wavefunctions to our "near-equilibrium" wavefunction, they did not equilibrate over the time scales we were considering. The PGPE requires nonlinear interactions in the C-region and an excess of energy over the ground state to thermalise — and thus for "cold" systems the PGPE did not equilibrate. This means that the dynamics we observed may have been affected by the choice of initial wavefunction.

With this in mind, we decided to study a second and more advanced c-field formalism: the *stochastic* PGPE.

Chapter 3

The Stochastic Projected Gross-Pitaevskii Equation

In this chapter I describe the *stochastic PGPE* (SPGPE) and its successful implementation. This provides us with a second tool for studying dipolar Bose gases, and I go on to explore what the SPGPE predicts about the behaviour of dipolar Bose gases at high temperatures.

3.1 The SPGPE

When we were first developing c-field techniques, we were presented with a choice as to which interactions we accounted for. Let us reconsider the possible interactions we can have between the C- and I-regions.

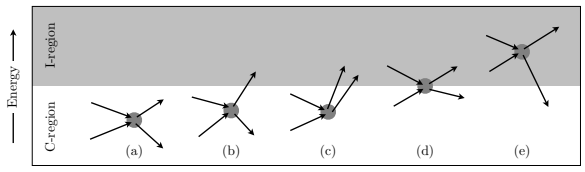

Repeat of Figure 2.2, which depicted the interaction terms that appear in the finite temperature GPE

For the PGPE, we chose to only account for interaction (a). The stochastic PGPE (SPGPE) is another c-field technique which accounts for interactions (a) and (e). In essence, the SPGPE no longer ignores the incoherent region, but treats it as an "infinite" thermal and particle reservoir. This requires the I-region to contain many weakly populated modes, meaning that the SPGPE is valid for sufficiently large systems for temperatures from about $0.5T_C$ to T_C. The SPGPE is a *grand canonical* approach: the C-region is evolved coupled to a reservoir with a chemical potential μ and temperature T.

Once a system has equilibrated via the SPGPE, it has no net particle or energy exchange with the reservoir. In these cases, the SPGPE and PGPE are roughly equivalent. However, the slow thermalisation of the PGPE was causing us difficulties in the

previous chapter. Additionally, we now want to be able to consider wavefunctions that are not necessarily near equilibrium. The SPGPE offers us a better tool for treating these systems.

An additional advantage of the SPGPE is the parameters we can now control. When using the PGPE, the temperature of the system was somehow related to the energy of the chosen initial wave function. And as I mentioned in the previous chapter, determining the temperature of a system in the PGPE framework is not entirely straightforward. In contrast, the SPGPE incorporates the temperature as a tunable parameter of the system, which is a distinct advantage.

SPGPE Theory

Compared to the PGPE, the SPGPE has a lot more underlying theory. To treat the interaction term (e), we must use Wigner phase space methods. I will not discuss this formalism here in any detail, but a comprehensive discussion of the SGPGE can be found in [32] and the precise details of the derivation are contained in [33, 34, 35, 36].

In brief, if we define the GPE operator

$$\mathcal{L} = -\frac{\hbar^2\nabla^2}{2m} + g|\psi|^2 + \Phi_D \tag{3.1}$$

then the (simple growth) SPGPE is

$$d\psi(\mathbf{x},t) = \mathcal{P}\left\{-\frac{i}{\hbar}\mathcal{L}\psi(\mathbf{x},t)dt + \frac{\gamma}{k_BT}(\mu-\mathcal{L})\psi(\mathbf{x},t)dt + \sqrt{2\gamma}dW(\mathbf{x},t)\right\} \tag{3.2}$$

where γ, μ, and T represent the coupling, chemical potential, and temperature of the reservoir and $\mathcal{P}$ is the C-region projection operator as before. But although we will not discuss this equation formally, we can gain some insight into what it says.

The first term is the familiar Hamiltonian operator for a Bose gas, in the same form as it appeared in the GPE and PGPE.

The second term contributes damping to the system. In the absence of the third term[1], the system would evolve until the chemical potential of the system is equal to the chosen value for the parameter μ. Note that this damping term disappears when $(\mu-\mathcal{L})\mathcal{P}\psi(\mathbf{x},t) = 0$, which is reminiscent of the time-independent PGPE equation.

The final term $dW(\mathbf{x},t)$ has come from the Wigner formalism. It contributes complex gaussian noise to the system from the reservoir, transferring energy and particles

[1]The case $dW = 0$ is known as the *quiet* PGPE

from the I- to the C-region.

3.2 Algorithm Validation; Density Distributions

Computationally, the SPGPE is implemented using a 4-5 Runge-Kutta algorithm, with an adaptive step size. At the end of each step, some noise is added using the Euler method.

Our SPGPE code builds on the dipolar PGPE code in the previous chapter. The main issues in validating the code are not whether the dipole-dipole interactions are implemented correctly, as we verfied this already for the PGPE. We want to determine is whether the noise and damping have been correctly implemented.

To do this, we considered the k-space density distribution of the gas when it is at equilibrium. By "k-space density distribution", I mean

$$N(\mathbf{k}) = \langle |\mathcal{F}(\psi(\mathbf{x}))|^2 \rangle \tag{3.3}$$

Before we begin discussing results from simulations, let us first predict what we will see at low temperatures.

In low temperature regimes, the Bogoliubov approximation is valid, and individual quasiparticle modes interact with the reservoir *independently* of one another. We therefore expect each quasiparticle mode to have a mean occupation of[2]

$$\langle \hat{\alpha}^\dagger_{\mathbf{k}} \hat{\alpha}_{\mathbf{k}} \rangle = \frac{k_B T}{\epsilon_k - \mu} \tag{3.4}$$

where $\epsilon_k - \mu$ is given by the Bogoliubov dispersion relation $E_k = \sqrt{\epsilon^0_k(\epsilon^0_k + 2n\tilde{V}(\mathbf{k}))}$, since the Bogoliubov energies are defined relative to the condensate chemical potential.

We must deduce what equation 3.4 implies for the plane-wave operators $\hat{a}_k$, as it is in a plane-wave basis that we consider our system numerically. Recall that we defined the quasiparticle operators as

$$\begin{aligned} \hat{a}_{\mathbf{k}} &= u_k \hat{\alpha}_{\mathbf{k}} - v_k \hat{\alpha}^\dagger_{-\mathbf{k}} \\ \hat{a}^\dagger_{-\mathbf{k}} &= u_k \hat{\alpha}^\dagger_{-\mathbf{k}} - v_k \hat{\alpha}_{\mathbf{k}} \end{aligned} \tag{3.5}$$

[2]The reader may rightfully ask why we have not used the Bose-Einstein distribution here. The SPGPE assumes that the occupation of the modes in the C-region have an occupation much larger than unity. Because of this, we expect the mean occupation of any given mode to be given not by the Bose-Einstein distribution, but by *classical limit* of the Bose-Einstein distribution — that is, equipartition.

It follows from these definitions that

$$\hat{a}^\dagger_{\mathbf{k}}\hat{a}_{\mathbf{k}} = u_k^2\hat{\alpha}^\dagger_{\mathbf{k}}\hat{\alpha}_{\mathbf{k}} - u_k v_k(\hat{\alpha}_{-\mathbf{k}}\hat{\alpha}_{\mathbf{k}} + \hat{\alpha}^\dagger_{\mathbf{k}}\hat{\alpha}_{-\mathbf{k}}) + v_k^2\hat{\alpha}_{-\mathbf{k}}\hat{\alpha}^\dagger_{-\mathbf{k}} \tag{3.6}$$

Taking averages, we obtain

$$\langle\hat{a}^\dagger_{\mathbf{k}}\hat{a}_{\mathbf{k}}\rangle = \langle\hat{\alpha}^\dagger_{\mathbf{k}}\hat{\alpha}_{\mathbf{k}}\rangle u_k^2 + (\langle\hat{\alpha}^\dagger_{-\mathbf{k}}\hat{\alpha}_{-\mathbf{k}}\rangle + 1)v_k^2 \tag{3.7}$$

The ensemble averages $\langle\hat{\alpha}_{-\mathbf{k}}\hat{\alpha}_{\mathbf{k}}\rangle$ and $\langle\hat{\alpha}^\dagger_{\mathbf{k}}\hat{\alpha}_{-\mathbf{k}}\rangle$ vanished because the quasiparticle operators were defined to remove non-diagonal terms from the Hamiltonian.

Additionally, in the classical limit the commutator $[\hat{\alpha}^\dagger_{\mathbf{k}}, \hat{\alpha}_{\mathbf{k}}]$ is negligible, so using equation 3.4 we arrive at the final result

$$N(\mathbf{k}) = \langle\hat{a}^\dagger_{\mathbf{k}}\hat{a}_{\mathbf{k}}\rangle \cong (u_k^2 + v_k^2)\frac{k_B T}{E_k} \tag{3.8}$$

This is the k-space density distribution we expect our system to obey. Since we used Bogoliubov theory in its derivation, it should only hold at low temperatures, where quasiparticle interactions are negligible.

The Noninteracting Gas

To confirm our SPGPE code was working correctly, we first considered the noninteracting gas ($g = g_{dd} = 0$). In this case the non-interacting plane wave modes are themselves the quasiparticles.[3] Thus the plane wave modes themselves should obey the distribution $\frac{k_B T}{E_k}$. Knowing this, we simulated the non-interacting gas at low temperatures. The results of these simulations are displayed in Figure 3.2.

[3] One can show explicitly that in the noninteracting case we have $u_k = 1$, $v_k = 0$

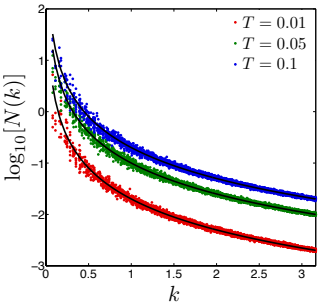

Figure 3.2: Mode occupation for a non-interacting gas evolved using the SPGPE with $\mu = 10^{-4}$. The average mode occupation as found by our code is plotted in red, green and blue for three different low reservoir temperatures. The black lines show the theoretical distributions as given by equation 3.8, which are well matched by the data.

It is important to note that we would expect the SPGPE to predict a classical distribution even in those cases where the system has very few excitations. Recall that c-field techniques assume that the modes in the C-region are macroscopically occupied. In these low energy cases, this assumption is invalid, so when we apply the SPGPE to these systems, we do so erroneously. This is reflected in the fact that the SPGPE returns not the Bose-Einstein distribution, but its classical limit.

Because the SPGPE code returned the classical distribution we had confidence that the algorithm was functioning correctly for the non-interacting case.

The Interacting Gas

With more confidence in my SPGPE implementation, we now reintroduce both contact and dipolar interactions to the system, and consider the effect of temperature on $N(k)$. We did this for the three cases from Figure 2.3 — the "contact", "weakly dipolar", and "strongly dipolar" cases we previously studied using the PGPE. The results for the weakly dipolar case are shown in Figure 3.3.

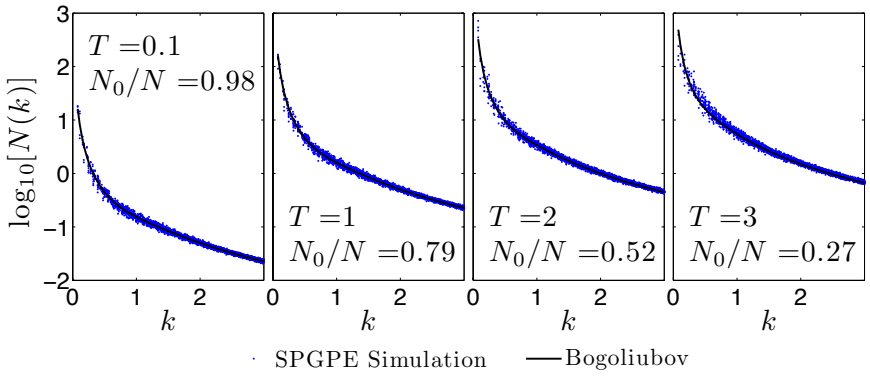

Figure 3.3: k-space density distributions $N(k)$ in the weakly dipolar case.

From this figure, it is evident that the density profile does not significantly differ from the Bogoliubov theory, at low temperatures, demonstrating that our SPGPE method is working in the interacting regime. Furthermore, the theories continued to agree even at high temperatures.

We saw good agreement with Bogoliubov theory for the contact and strongly dipolar cases, too. The distribution was changed very little[4] by dipolar interactions.

[4]We do see a "bump" in the strongly dipolar profile, corresponding to the "halo" we saw for rotonic systems in Chapter 2. However, this bump was very small and would be incredibly hard to measure.

3.3 Density Fluctuations

As we just discussed, the density distributions $N(k)$ were not drastically affected by introducing dipolar interactions. In light of this, we now turn to a quantity that should be much more sensitive to interactions: *density fluctuations*. We define

$$\delta n_k = \mathcal{F}\left(n(\mathbf{x}) - \overline{n}\right) \tag{3.9}$$

as the spatial spectrum of density fluctuations, which are characterised by the expectation

$$S(k) = \frac{\langle |\delta n_k|^2 \rangle}{N} \tag{3.10}$$

The quantity $S(k)$ is a measure of the density fluctuations, and is known as the static structure factor. The division by N (the total particle number) ensures it is conventionally normalised. As it can be seen from its definition, the density fluctuations are a k-space decomposition of the fluctuations in the system's density.

It is already known that the density fluctuations of a gas differ notably between contact and dipolar gases. Density fluctuations have been identified as a possible "signature" for dipolar interactions [37].

Importantly, density fluctuations have been experimentally measured using *in situ* imaging [38] and by Bragg spectroscopy [39], so they are a reasonable parameter to consider.

As always, we will want to compare our simulation results to preexisting theory, so before carrying out simulations we will first consider some theoretical predictions.

Bogoliubov Treatment of Density Fluctuations

We now construct what Bogoliubov theory predicts for the density fluctuations. Again, let us adopt the plane-wave basis

$$\hat{\psi}(\mathbf{x}) = \sum_{\mathbf{k}} \frac{1}{L} e^{i\mathbf{k}\cdot\mathbf{x}} \hat{a}_{\mathbf{k}} \tag{3.11}$$

In this basis, the corresponding operator $\hat{n}(\mathbf{x}) = \hat{\psi}^\dagger(\mathbf{x})\hat{\psi}(\mathbf{x})$ can be written as

$$\hat{n}(\mathbf{x}) = \frac{1}{L^2} \sum_{\mathbf{q}} e^{i\mathbf{q}\cdot\mathbf{x}} \hat{N}_{\mathbf{q}} \tag{3.12}$$

where

$$\hat{N}_{\mathbf{q}} = \sum_{\mathbf{k}} \hat{a}^{\dagger}_{\mathbf{k}-\mathbf{q}} \hat{a}_{\mathbf{k}} \tag{3.13}$$

Now, if we adopt the Bogoliubov prescription $\hat{a}_0,\ \hat{a}_0^{\dagger} \to \sqrt{N_0}$, we can separate $\hat{N}_{\mathbf{q}}$ into terms proportional to N_0, $\sqrt{N_0}$ and 1. Since $N_0 \gg 1$, these terms get progressively smaller. To order $\sqrt{N_0}$, equation 3.13 becomes

$$\hat{N}_{\mathbf{q}} \approx N_0 + \sqrt{N_0}(\hat{a}^{\dagger}_{-\mathbf{q}} + \hat{a}_{\mathbf{q}}) = N_0 + \sqrt{N_0}(u_q - v_q)(\hat{\alpha}^{\dagger}_{-\mathbf{q}} + \hat{\alpha}_{\mathbf{q}}) \tag{3.14}$$

If we substitute equation 3.14 back into equation 3.12, it can be seen that the density fluctuations of the gas (in real space) are given by

$$\delta\hat{n}(\mathbf{x}) = \hat{n}(\mathbf{x}) - \overline{n} = \frac{\sqrt{N_0}}{L^2} \sum_{\mathbf{q}\neq 0} e^{i\mathbf{q}\cdot\mathbf{x}}(u_q - v_q)(\hat{\alpha}^{\dagger}_{-\mathbf{q}} + \hat{\alpha}_{\mathbf{q}}) \tag{3.15}$$

where we have set $\overline{n} = N_0/L^2$. In Fourier space, these density fluctuations become

$$\begin{aligned} \delta\hat{n}_{\mathbf{k}} &= \int d\mathbf{x}\ e^{i\mathbf{k}\cdot\mathbf{x}}\ \delta\hat{n}(\mathbf{x}) \\ &= \sqrt{N_0}(u_k - v_k)(\hat{\alpha}^{\dagger}_{\mathbf{k}} + \hat{\alpha}_{-\mathbf{k}}) \end{aligned} \tag{3.16}$$

Thus

$$\langle \delta\hat{n}^{\dagger}_{\mathbf{k}} \delta\hat{n}_{\mathbf{k}} \rangle = N_0(u_k - v_k)^2 \langle (\hat{\alpha}_{\mathbf{k}} + \hat{\alpha}^{\dagger}_{-\mathbf{k}})(\hat{\alpha}^{\dagger}_{\mathbf{k}} + \hat{\alpha}_{-\mathbf{k}}) \rangle \tag{3.17}$$

Noting that some of the ensemble averages disappear, we find that[5]

$$S(k) \coloneqq \frac{\langle |\delta\hat{n}_{\mathbf{k}}|^2 \rangle}{N_0} = (u_k - v_k)^2 (\langle \hat{\alpha}^{\dagger}_{\mathbf{k}} \hat{\alpha}_{\mathbf{k}} \rangle + \langle \hat{\alpha}^{\dagger}_{-\mathbf{k}} \hat{\alpha}_{-\mathbf{k}} \rangle + 1) \tag{3.18}$$

In the classical limit the commutator is negligible and ensemble averages are given by the limit of the Bose-Einstein distribution (much like when we were considering density distributions). Therefore we obtain the final result

$$S(k) = (u_k - v_k)^2 \frac{2k_B T}{E_k} \tag{3.19}$$

[5]The reader may notice that I here divide by N_0, but when I originally introduced density fluctuations in equation 3.10, I divided by N. In the Bogoliubov case, $N_0 \cong N$. But we will soon consider higher temperatures where the condensate number will drop significantly below N. At these higher temperatures, N is the appropriate divisor.

Simulations

Having established a theoretical expression for density fluctuations in the Bogoliubov regime, we are ready to consider some simulations.

Density fluctuations are ideally measured when the system is at equilibrium. We therefore started with a "top hat" wavefunction, and allowed it to evolve until it equilibrated. We then periodically measured $\delta\hat{n}_{\mathbf{k}}$ as the system evolved while in equilibrium. The density fluctuations can then be calculated using the average of this set of accumulated measurements $\{\delta\hat{n}_{\mathbf{k}}\}$.

Figure 3.4 illustrates two typical density fluctuation results.

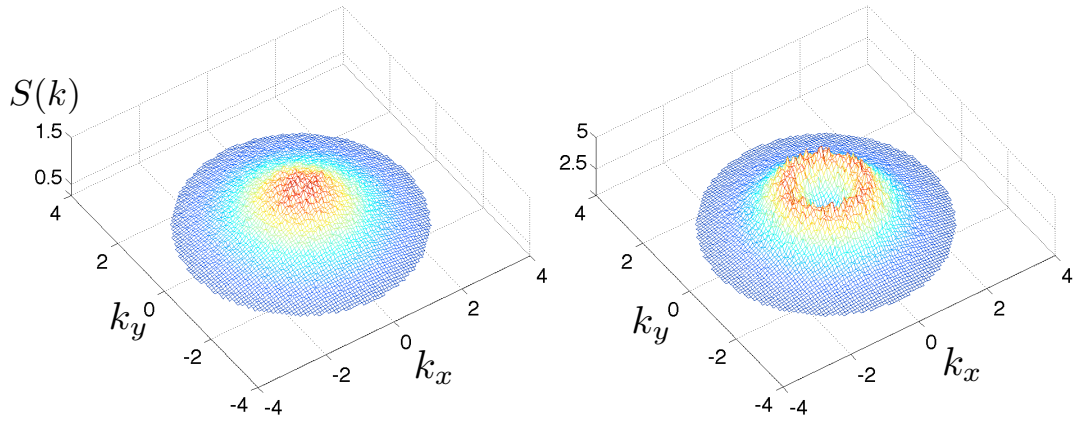

Figure 3.4: Density fluctuations at $T = \mu = \gamma = 1$ for the "contact" ($g = 0.25$, $g_{dd} = 0$) case and a "moderately" dipolar system ($g = 0$, $g_{dd} = 0.125$), averaged over a time of $\sim 200\tau$ and for a system with $L = 80$ and $\epsilon_{cut} = 5$.

In contrast to the density distributions, there is a very clear difference between these two sets of results. The contact distribution appears much like a "hill", whereas the dipolar distribution becomes a "volcano" with a peak in density fluctuations for near-rotonic wavelengths. It seems that it is very favourable for these modes to fluctuate. This volcano-like distribution is characteristic of dipolar systems. It is also important to note that the maximum fluctuation value is more than *three times larger* in the dipolar case.

Let us study these results in more detail. We are specifically interested how the density fluctuations are dependent on temperature. At low temperatures, the SPGPE and Bogoliubov theories should predict similar density fluctuations. However, at higher temperatures the Bogoliubov treatment becomes invalid. In these regimes, the c-field

predictions should begin to disagree with the predictions of Bogolibov theory, and the SPGPE should provide some insight into the effects of quasiparticle interactions. We examine the temperature dependence of density fluctuations in Figure 3.5.

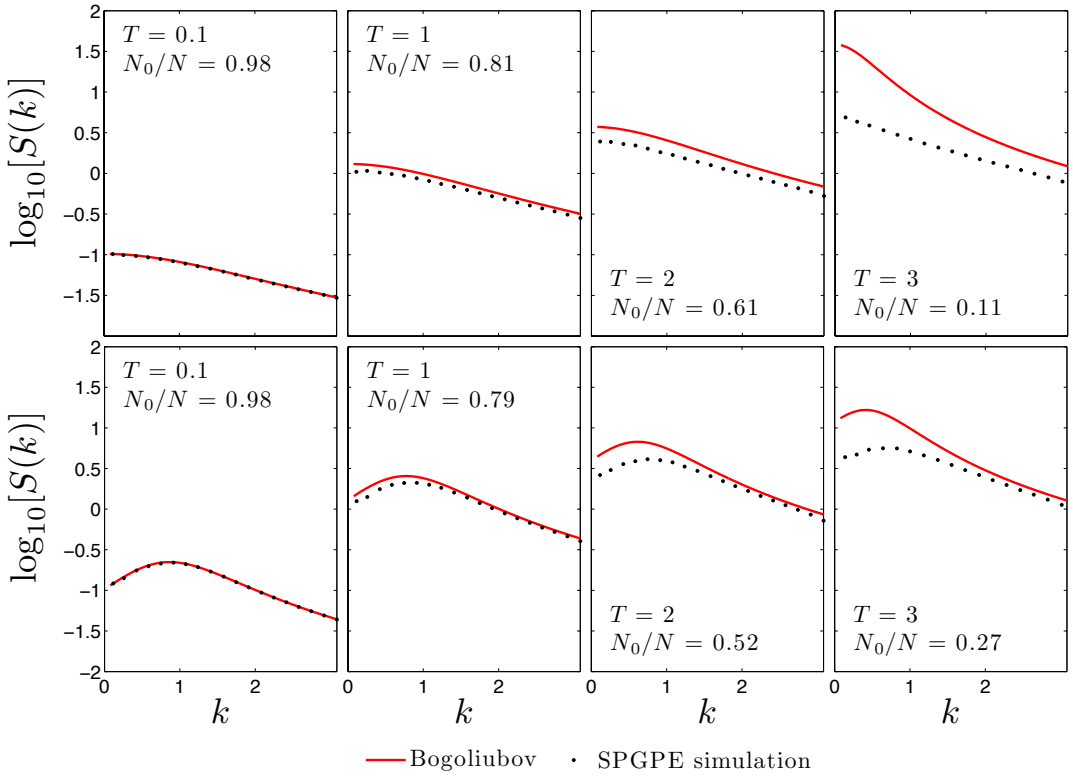

Figure 3.5: Density fluctuations as a function of $k = \sqrt{k_x^2 + k_y^2}$ for the contact (top row) and weakly dipolar cases (bottom row). Each set of simulation data is simply the radial profile of a distribution much like those of Figure 3.4. (One can picture rotating these graphs about the $k = 0$ axis to recover "hills" and "volcanoes".) The parameters chosen for these simulations were $\mu = \gamma = 1$, $L = 80$, and $\epsilon_{cut} = 5$, and the fluctuations were measured over a time span of $\sim 200\tau$.

As suspected, we witness a departure of the SPGPE from Bogoliubov theory: in both cases, the SPGPE predicts significantly lower density fluctuations at low k values.

These are the results for the "contact" and "weakly dipolar" case. As I attempted to obtain the same results for the strongly dipolar case, we witnessed a familiar instability: the "pimple" features resurfaced.

For the strongly dipolar case, the simulations were incredibly temperamental, breaking down at temperatures as low as $T = 0.1$. As they did in the case of the PGPE, these pimples prevented us from considering high temperature, strongly dipolar systems. As a concession, we weakened the dipolar effects to consider a system with a "moderate" dipolar strength (lying in between the "weakly" and "strongly" dipolar cases we've been considering). However, even this system showed some instabilities for $T \gtrsim 1$, which are shown in Figure 3.6.

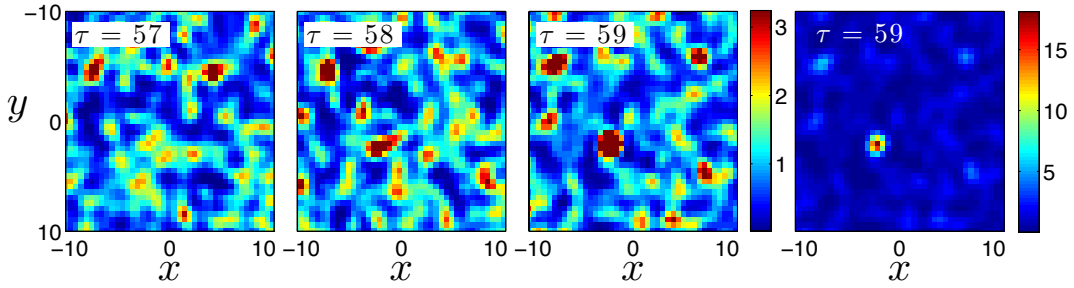

Figure 3.6: Snapshots of the position space density of a "moderately" dipolar gas evolving via the SPGPE at $T = 1.5$. In the space of these three time steps, a "pimple" appears, and very shortly after $\tau = 59$ the code broke down.

Of course, one would not turn to the SPGPE to try to avoid these pimples forming (and this was not our primary motivation for leaving the PGPE). The pimples, as we have discussed, are regions of incredibly high density that grow dramatically, pulling more of the surrounding gas into itself. Because the SPGPE has introduced coupling with an "infinite" particle reservoir, this growth is now even more dramatic; the pimple can grow even faster by drawing particles from the reservoir. This made the appearance of pimples even more calamitous; upon pimple formation, the Runge-Kutta algorithm almost immediately broke down (no step size, no matter how small, would return a result within the the algorithm's error tolerance).

We will not pursue the strongly dipolar (rotonic) regime here.[6]

[6]We note that by working in the larger condensate regime (keeping $\mu = n(g + 2g_{dd})$ constant but increasing n and decreasing $g + 2g_{dd}$ we expect the instability to be less troublesome.

3.4 An Upper Bound on the Dispersion

As already discussed, the density fluctuations of a gas are dramatically affected by dipolar interactions and thus serve as a signature of the dipole-dipole interaction.

Furthermore, the usefulness of knowing $S(k)$ extends beyond knowing how the gas will fluctuate.

When we considered elementary excitations of the zero temperature dipolar Bose gas in Section 1.5, we acquired the dispersion relation

$$E_k = \sqrt{\epsilon_k^0(\epsilon_k^0 + 2n\tilde{V}(\mathbf{k}))} \tag{3.20}$$

where $\epsilon_k^0 = \frac{\hbar^2 k^2}{2m}$ is the single particle energy, n is the particle density and $\tilde{V}(\mathbf{k})$ is the interaction potential in Fourier space.

This expression for the dispersion only holds where the Bogoliubov approximation is valid (namely, when the thermal depletion is small). As we push upwards to higher temperatures, the dispersion relation itself will be affected and we cannot expect equation 3.20 to be accurate.

Calculating the dispersion relation at non-zero temperatures is a difficult task. However, because we know how $S(k)$ behaves at higher temperatures, we are in a position to gain some insight into how the dispersion relation has shifted. This is what we will investigate now.

In his studies of liquid helium, Feynman proposed [40] that the dispersion relation has an upper bound given by

$$E_k \leqslant \frac{\epsilon_k^0}{S(k)} \tag{3.21}$$

(He obtained this result via a variational approach.) Equation 3.21 only applies at zero temperature, but it can be generalised to nonzero temperatures [41] as

$$\omega(k) \leqslant \omega_F(k) \qquad \text{where} \qquad \hbar\omega_F(k)\tanh\left(\frac{\hbar\omega_F(k)}{2k_BT}\right) = \frac{\epsilon_0^k}{S(k)} \tag{3.22}$$

which in the classical limit (leading to equipartition) becomes

$$\frac{\hbar^2\omega_F^2(k)}{2k_BT} = \frac{\epsilon_0^k}{S(k)} \tag{3.23}$$

To get an appreciation as to where this is coming from, let us reconsider the Bogoliubov

prediction for density fluctuations. This was given by equation 3.19 as

$$S(k) = (u_k - v_k)^2 \frac{2k_B T}{E_k} \tag{3.24}$$

where E_k is the Bogoliubov dispersion. We know explicitly what u_k and v_k are in terms of ϵ_k^0 and $n\tilde{V}(\mathbf{k})$ (see equation A.27). Using these definitions, we can expand these coefficients to show that

$$(u_k - v_k)^2 = \frac{\epsilon_k^0}{E_k} \tag{3.25}$$

and thus equation 3.24 becomes

$$S(k) = \frac{2\epsilon_k^0 k_B T}{E_k^2} \Longrightarrow E_k = \sqrt{\frac{2\epsilon_0^k k_B T}{S(k)}} \tag{3.26}$$

Note that this matches equation 3.23. However, in that result $\omega_F(k)$ was an *upper bound* on the dispersion, not the dispersion itself. It just so happens that in the Bogoliubov limit the dispersion ω is equal to the upper bound ω_F.

In conclusion, we can infer an upper bound for the system's dispersion relation given by

$$E_k \leqslant \sqrt{\frac{2\epsilon_0^k k_B T}{S(k)}} \tag{3.27}$$

In the previous section, we obtained a new (and hopefully improved) $S(k)$ via SPGPE simulations. We can now use those results to derive a new upper bound on E_k (see Figures 3.7 and 3.8).

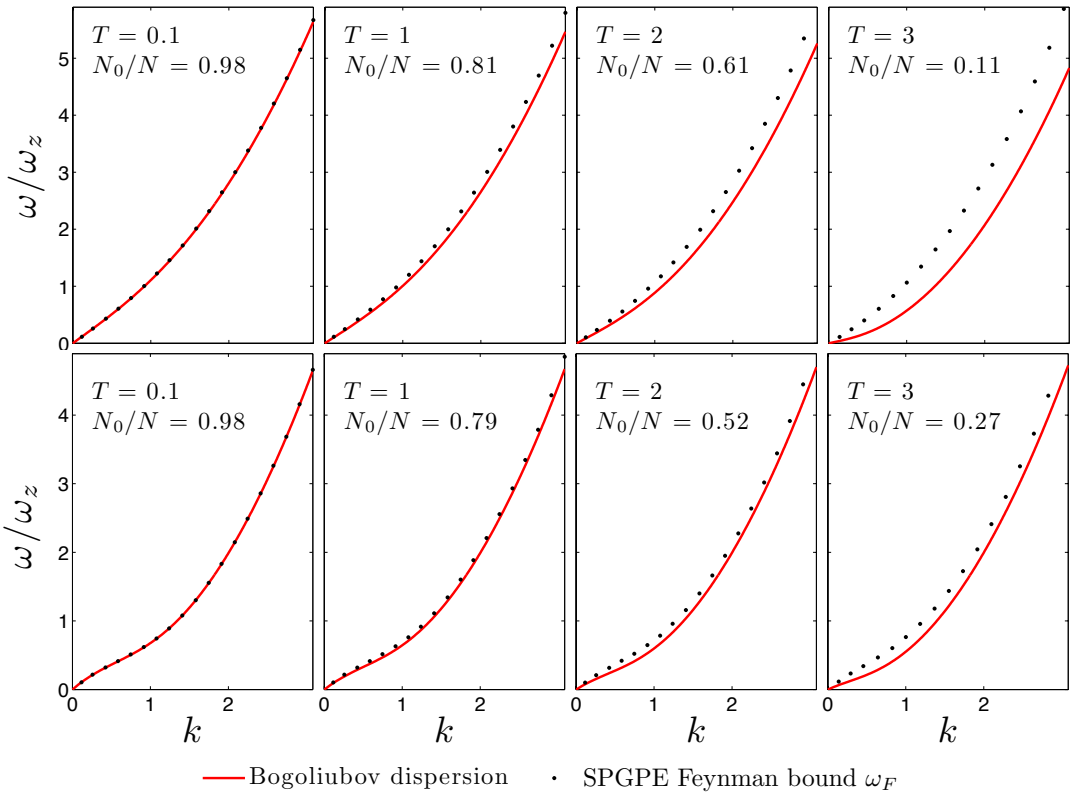

Figure 3.7: Dispersion relations for the contact (top row) and weakly dipolar cases (bottom row). The Bogoliubov dispersion relation is plotted in red, while in black we have the new upper bound as calculated using the SPGPE density fluctuation results. These plots were obtained for the same parameters as Figure 3.5.

For the contact and weakly dipolar cases, the "pimples" did not trouble us, and we were able to consider the high temperature regimes of interest. As expected, the Bogoliubov and SPGPE Feynman limit agree at low temperatures, and at higher temperatures, they part, with the SPGPE predicting upper bounds that are higher than what Bogoliubov theory proposes. Interestingly, the dipolar case is closer to the Bogoliubov dispersion than the contact case.

Unfortunately, the appearance of the instabilities completely prevented us from studying the strongly dipolar regime. However, we did investigate the "moderately dipolar" case; the results for which are shown in Figure 3.8.

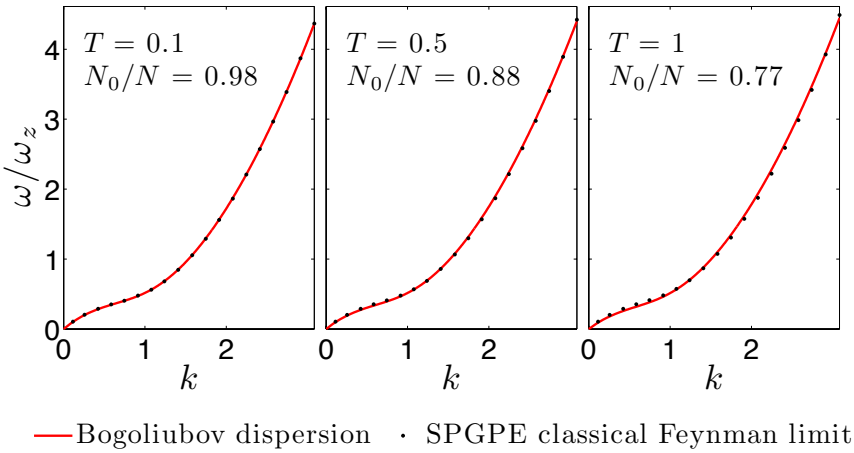

Figure 3.8: Dispersion relation for the moderately dipolar case. These were obtained for the same parameters as Figure 3.5, but with $g = 0$, $g_{dd} = 0.125$.

These results are still for low temperatures, so by $T = 1$ we do not yet see substantial change in the dispersion. However, what small disagreements we do see hint at a possible increase in the dispersion for low k modes, whcih would suggest these modes are more robust than Bogoliubov theory indicates. But more importantly, we also see suggestions of a decrease at more energetic modes, suggesting these modes are softened by their interaction with other quasiparticles. This is quite different from the raised dispersions in the contact and weakly dipolar cases, where the higher modes increased in energy. In light of this, one might boldly speculate that for stronger dipolar cases the dispersion will lower at high k.

Conclusion and Future Work

In summary, the significant achievements of this work are as follows:

Implementation of the PGPE and SPGPE for quasi-2D dipolar systems

We successfully made the first implementation of the PGPE and SPGPE for quasi-2D dipolar gases. In this dissertation, I have described this implementation and the extensive validation of our algorithm that we carried out.

Having read this dissertation, it may appear to the reader that the only options for theoretically considering Bose gases are either Bogoliubov theory or c-field techniques. Of course, this is not the case. There are a number of methods for considering these systems[1].

A standard procedure for treating non-zero temperature BECs is the Hartree-Fock-Bogoliubov-Popov (HFBP) formalism. The HFBP is an improvement upon the Bogoliubov approximation, and has been widely used in the case of Bose gases with contact interactions. However, incorporating long-range interactions into the HFBP is a challenge. It is particularly difficult to incorporate the thermal exchange interaction[2] For this reason, the HFBP is not ideal for considering the dipole-dipole interaction.

We encountered no such difficulties when using c-field techniques — these methods are better suited to handling long-range interactions. For this reason, our success in implementing these c-field methods for dipolar interactions is an important achievement.

Identifying Roton Regime Instability

Having implemented c-field techniques, we explored the behaviour of dipolar gases, and quickly discovered system instabilities. In the rotonic regime, the system appears highly sensitive to thermal fluctuations, even for systems with very small thermal fractions. This behaviour is not apparent from Bogoliubov theory.

These instabilities, which appeared in both the PGPE and SPGPE simulations, are of substantial interest. Currently, there is a lot of attention in the dipolar BEC

[1] For an in-depth discussion about some of these techniques, see [42]

[2] Recall that the exchange interaction is the interaction between two identical particles arising from symmetrisation of the wavefunction. The *thermal* exchange interaction is concerned with the exchange interaction of particles outside the condensate (hence "thermal").

community focused on the stability of these condensates. With experiments currently searching for evidence of rotons in dipolar BECs, our initial findings suggest it may be difficult to obtain equilibrium systems in the roton regime.

Study of Density Fluctuations

We obtained the density fluctuations for the contact and weakly dipolar regimes, and there were dramatic differences in the density fluctuation profiles for these two cases. Furthermore, we also found that c-field techniques suggested density fluctuations will be smaller than Bogoliubov theory predicts. These differences are something that experiments could explore.

The density fluctuations we obtained also provided some insight into the dispersion relation of the system.

From here, there are a number of possible avenues for further work.

We identified system instabilities of significant interest — but we have only noted their appearance. Characterising collapse and studying the lead-up to collapse could be worthwhile. This may allow us to assess the time window in which it might be practical to detect rotons.

In further study of the instabilities, it would be interesting to incorporate three-body loss terms into our equations of motion. Three body loss leads to particle loss in regions of high density, and this action may combat the local density peaks seen during collapse.

It would also be worthwhile to consider better methods for inferring the dispersion relation of our system. The Feynman limit we considered is an upper bound, and can be a fairly poor estimate for the actual dispersion. If we are indeed witnessing rotonic collapse, the dispersion ought to be approaching zero. There exist better methods for extracting the dispersion relation of the system, and these improved dispersions may tell a different story.

If we were not interested in the collapse, but instead desired to study the density distributions and dispersions for the rotonic regime, we could avoid the instabilities by working in the larger condensate regime (for example, by keeping $\mu = n(g + 2g_{dd})$ constant but increasing n and decreasing $g + 2g_{dd}$). This way, we should be able to obtain stable rotonic systems.

It would also be worthwhile comparing our results found in this dissertation (such as density fluctuations) to other non-zero temperature theories such as HFBP. Making

these comparisons could verify what we have seen — or possibly force us to consider and resolve any differences between the two theories, should they arise.

Finally, our system may provide a method for evaluating thermal exchange interactions for large systems. As such, existing studies using self-consistent mean field calculations have only been able to consider small systems and are computationally very expensive [43, 44]. Our techniques can treat large systems and make including thermal exchange interactions tractable.

References

[1] A. Griesmaier, J. Werner, S. Hensler, J. Stuhler, and T. Pfau, "Bose-Einstein condensation of chromium," *Phys. Rev. Lett.*, vol. 94, p. 160401, Apr 2005.

[2] M. Lu, N. Q. Burdick, S. H. Youn, and B. L. Lev, "Strongly dipolar Bose-Einstein condensate of dysprosium," *Phys. Rev. Lett.*, vol. 107, p. 190401, Oct 2011.

[3] K. Aikawa, A. Frisch, M. Mark, S. Baier, A. Rietzler, R. Grimm, and F. Ferlaino, "Bose-Einstein condensation of erbium," *Phys. Rev. Lett.*, vol. 108, p. 210401, May 2012.

[4] T. Koch, T. Lahaye, J. Metz, B. Frhlich, A. Griesmaier, and T. Pfau, "Stabilization of a purely dipolar quantum gas against collapse," *Nature Physics*, vol. 4, no. 3, p. 218222, 2008.

[5] T. Lahaye, J. Metz, B. Fröhlich, T. Koch, M. Meister, A. Griesmaier, T. Pfau, H. Saito, Y. Kawaguchi, and M. Ueda, "d-wave collapse and explosion of a dipolar Bose-Einstein condensate," *Phys. Rev. Lett.*, vol. 101, p. 080401, Aug 2008.

[6] A. Chotia, B. Neyenhuis, S. A. Moses, B. Yan, J. P. Covey, M. Foss-Feig, A. M. Rey, D. S. Jin, and J. Ye, "Long-lived dipolar molecules and Feshbach molecules in a 3D optical lattice," *Phys. Rev. Lett.*, vol. 108, p. 080405, Feb 2012.

[7] K. Aikawa, D. Akamatsu, M. Hayashi, K. Oasa, J. Kobayashi, P. Naidon, T. Kishimoto, M. Ueda, and S. Inouye, "Coherent Transfer of Photoassociated Molecules into the Rovibrational Ground State," *Physical Review Letters*, vol. 105, p. 203001, Nov. 2010.

[8] M. Vengalattore, S. R. Leslie, J. Guzman, and D. M. Stamper-Kurn, "Spontaneously modulated spin textures in a dipolar spinor Bose-Einstein condensate," *Phys. Rev. Lett.*, vol. 100, p. 170403, May 2008.

[9] T. Lahaye, C. Menotti, L. Santos, M. Lewenstein, and T. Pfau, "The physics of diploar bosonic quantum gases," *Reports on Progress in Physics*, vol. 72, p. 126401, 2009.

[10] S. Müller, J. Billy, E. A. L. Henn, H. Kadau, A. Griesmaier, M. Jona-Lasinio, L. Santos, and T. Pfau, "Stability of a dipolar Bose-Einstein condensate in a one-dimensional lattice," *Phys. Rev. A*, vol. 84, p. 053601, Nov 2011.

[11] D. S. Petrov, M. Holzmann, and G. V. Shlyapnikov, "Bose-Einstein condensation in quasi-2D trapped gases," *Phys. Rev. Lett.*, vol. 84, pp. 2551–2555, Mar 2000.

[12] L. Pitaevskii and S. Stringari, *Bose-Einstein Condesation.* Oxford University Press, 2003.

[13] E. Gross, "Structure of a quantized vortex in boson systems," *Il Nuovo Cimento Series 10*, vol. 20, no. 3, pp. 454–477, 1961.

[14] L. P. Pitaevskii, "Vortex lines in an imperfect Bose gas," *Sov. Phys. JETP*, vol. 13, p. 451, 1961.

[15] N. N. Bogoliubov, "On the theory of superfluidity," *J. Phys. (USSR)*, vol. 11, p. 23, 1947.

[16] E. Tiesinga, A. J. Moerdijk, B. J. Verhaar, and H. T. C. Stoof, "Conditions for Bose-Einstein condensation in magnetically trapped atomic cesium," *Phys. Rev. A*, vol. 46, pp. R1167–R1170, Aug 1992.

[17] S. Inouye, M. R. Andrews, J. Stenger, H.-J. Miesner, D. M. Stamper-Kurn, and W. Ketterle, "Observation of Feshbach resonances in a Bose-Einstein condensate," *Nature*, vol. 392, no. 6672, pp. 151–154, 1998.

[18] S. Giovanazzi, A. Görlitz, and T. Pfau, "Tuning the dipolar interaction in quantum gases," *Phys. Rev. Lett.*, vol. 89, p. 130401, Sep 2002.

[19] P. B. Blakie, D. Baillie, and R. N. Bisset, "Roton spectroscopy in a harmonically trapped dipolar Bose-Einstein condensate," *Phys. Rev. A*, vol. 86, p. 021604, Aug 2012.

[20] L. D. Landau, "On the theory of superfluidity in helium II," *J. Phys. (USSR)*, vol. 11, p. 91, 1947.

[21] D. G. Henshaw and A. D. B. Woods, "Modes of atomic motions in liquid helium by inelastic scattering of neutrons," *Phys. Rev.*, vol. 121, pp. 1266–1274, Mar 1961.

[22] P. Nozières, "Is the roton in superfluid 4He the ghost of a Bragg spot?," *Journal of Low Temperature Physics*, vol. 137, no. 1-2, pp. 45–67, 2004.

[23] M. J. Davis, R. J. Ballagh, and K. Burnett, "Dynamics of thermal Bose fields in the classical limit," *Journal of Physics B: Atomic, Molecular and Optical Physics*, vol. 34, no. 22, p. 4487, 2001.

[24] M. J. Davis, S. A. Morgan, and K. Burnett, "Simulations of thermal Bose fields in the classical limit," *Phys. Rev. A*, vol. 66, p. 053618, Nov 2002.

[25] J. Scott Russell, "Report on waves." Fourteenth meeting of the British Association for the Advancement of Science, 1844.

[26] J. Boussinesq, "Théorie de l'intumescence lliquid appelée onde solitaire ou de translation, se propageant dans un canal rectangulaire," *Compte Rendus Acad. Sci. Paris*, vol. 72, pp. 755–9, 1871.

[27] Lord Rayleigh, "On waves," *Philosophical Magazine (5)*, vol. 1, pp. 257–79, 1876.

[28] J. Denschlag, J. E. Simsarian, D. L. Feder, C. W. Clark, L. A. Collins, J. Cubizolles, L. Deng, E. W. Hagley, K. Helmerson, W. P. Reinhardt, S. L. Rolston, B. I. Schneider, and W. D. Phillips, "Generating solitons by phase engineering of a Bose-Einstein condensate," *Science*, vol. 287, no. 5450, pp. 97–101, 2000.

[29] P. Pedri and L. Santos, "Two-dimensional bright solitons in dipolar Bose-Einstein condensates," *Phys. Rev. Lett.*, vol. 95, p. 200404, Nov 2005.

[30] R. Nath, P. Pedri, and L. Santos, "Phonon instability with respect to soliton formation in two-dimensional dipolar Bose-Einstein condensates," *Phys. Rev. Lett.*, vol. 102, p. 050401, Feb 2009.

[31] A. Boudjemâa and G. V. Shlyapnikov, "Two-dimensional dipolar Bose gas with the roton-maxon excitation spectrum," *Phys. Rev. A*, vol. 87, p. 025601, Feb 2013.

[32] P. Blakie, A. Bradley, M. Davis, R. Ballagh, and C. Gardiner, "Dynamics and statistical mechanics of ultra-cold Bose gases using c-field techniques," *Advances in Physics*, vol. 57, no. 5, pp. 363–455, 2008.

[33] C. W. Gardiner, J. R. Anglin, and T. I. A. Fudge, "The stochastic Gross-Pitaevskii equation," *Journal of Physics B: Atomic, Molecular and Optical Physics*, vol. 35, no. 6, p. 1555, 2002.

[34] C. W. Gardiner and M. J. Davis, "The stochastic Gross-Pitaevskii equation: II," *Journal of Physics B: Atomic, Molecular and Optical Physics*, vol. 36, no. 23, p. 4731, 2003.

[35] A. Bradley and C. Gardiner, "The stochastic Gross-Pitaevskii equation: III." arXiv:cond-mat/0602162, Feb 2006.

[36] A. S. Bradley, C. W. Gardiner, and M. J. Davis, "Bose-Einstein condensation from a rotating thermal cloud: Vortex nucleation and lattice formation," *Phys. Rev. A*, vol. 77, p. 033616, Mar 2008.

[37] P. B. Blakie, D. Baillie, and R. N. Bisset, "Depletion and fluctuations of a trapped dipolar Bose-Einstein condensate in the roton regime," *Phys. Rev. A*, vol. 88, p. 013638, Jul 2013.

[38] C.-L. Hung, V. Gurarie, and C. Chin, "From cosmology to cold atoms: Observation of Sakharov oscillations in a quenched atomic superfluid," *Science*, vol. 341, no. 6151, pp. 1213–1215, 2013.

[39] I. Shammass, S. Rinott, A. Berkovitz, R. Schley, and J. Steinhauer, "Phonon dispersion relation of an atomic Bose-Einstein condensate," *Phys. Rev. Lett.*, vol. 109, p. 195301, Nov 2012.

[40] R. P. Feynman, "Atomic theory of the two-fluid model of liquid helium," *Phys. Rev.*, vol. 94, pp. 262–277, Apr 1954.

[41] A. Filinov, N. V. Prokof'ev, and M. Bonitz, "Berezinskii-Kosterlitz-Thouless transition in two-dimensional dipole systems," *Phys. Rev. Lett.*, vol. 105, p. 070401, Aug 2010.

[42] A. Griffin, T. Nikuni, and E. Zaremba, *Bose-Condensed Gases at Finite Temperatures*. Cambridge University Press, 2009.

[43] C. Ticknor, "Finite-temperature analysis of a quasi-two-dimensional dipolar gas," *Phys. Rev. A*, vol. 85, p. 033629, Mar 2012.

[44] S. C. Cormack and D. A. W. Hutchinson, "Finite-temperature dipolar ultracold Bose gas with exchange interactions," *Phys. Rev. A*, vol. 86, p. 053619, Nov 2012.

[45] U. R. Fischer, "Stability of quasi-two-dimensional Bose-Einstein condensates with dominant dipole-dipole interactions," *Phys. Rev. A*, vol. 73, p. 031602, Mar 2006.

[46] R. M. Wilson and J. L. Bohn, "Emergent structure in a dipolar Bose gas in a one-dimensional lattice," *Phys. Rev. A*, vol. 83, p. 023623, Feb 2011.

[47] A. L. Fetter, "Theory of a dilute low-temperature trapped Bose condensate," in *Proceedings of the International School of Physics Enrico Fermi*, 1998.

[48] S. Morgan, S. Choi, K. Burnett, and M. Edwards, "Nonlinear mixing of quasiparticles in an inhomogeneous Bose condensate," *Physical Review A*, vol. 57, no. 5, p. 3818, 1998.

[49] R. Wilson, *Manifestations of the Roton in Dipolar Bose-Einstein Condensates*. PhD thesis, University of Colorado, 2011.

Appendices

A.1 The Limitations to Quasi-2D

Quasi-2D geometry is really a limiting case of the oblate spherical trap — experimentally, the condensate necessarily needs to be confined in all directions. We make a number of assumptions in adopting a quasi-2D geometry. It is therefore important to know the applicability and limitations of these assumptions.

To have a quasi-2D geometry, recall that we required the following conditions to hold

$$k_B T \ll \hbar\omega_z \tag{A.1}$$

$$\mu \approx n_c(g + 2g_{dd}) \ll \hbar\omega_z \tag{A.2}$$

In this case, we asserted that $\psi(\mathbf{x}) = \chi(z)\psi(\boldsymbol{\rho})$, where $\chi(z)$ is the ground state of the harmonic oscillator

$$\chi(z) = \frac{1}{{l_z}^{1/2}\pi^{1/4}}\exp\left(-\frac{z^2}{2{l_z}^2}\right) \tag{A.3}$$

However, this ansatz is not entirely valid. Current dipolar experiments with flat "pancake" trap geometries do not quite satisfy these assumptions.

Furthermore, the conditions A.1 and A.2 are often pushed, if not broken, in many situations. In fact, in the case of repulsive contact interactions, roton collapse can only occur once the quasi-2D assumptions have already been violated [45].

All of this paints a fairly gloomy picture for quasi-2D, and any hope for obtaining useful information from quasi-2D models would appear faint. However, quasi-2D systems can in fact be qualitatively good models. Wilson *et al.* [46] considered an ultracold dipolar Bose gas in a one-dimensional lattice, as illustrated in Figure A.1.

Figure A.1: A one-dimensional lattice, consisting of stacked oblate wells. This is a typical experimental trap.

Wilson *et al.* then considered the validity of this ansatz by considering an alternative ansatz for the axial wavefunction

$$\chi(z) = \frac{1}{\sqrt{1-\lambda^2}} \left(\chi_0(z, l_z) + \lambda\chi_2(z, l_z)\right) \tag{A.4}$$

where l_z was now allowed to vary, χ_0 and χ_2 are the ground and second excited states of the harmonic potential, respectively, and λ is some parameter that defines the fraction of the wavefunction in the second excited state. This new anzatz allows the axial wavefunction to deform symmetrically. (They did not consider the first excited state, as its introduction would instead lead to translation.)

They then compared the results of simulations of three cases

- $\lambda = 0$ and l_z fixed (the standard quasi-2D assumption)
- both λ and l_z treated variationally
- full three-dimensional modelling

They found that while quantitatively the results of these simulations differed, *they exhibited the same behaviour qualitatively.*

This vindicates our choice to work in a quasi-2D geometry. So long as we keep in mind that our results may not be quantitatively accurate, quasi-2D models are very useful. Full three dimensional simulations of systems such as ours would be computationally very expensive. With quasi-2D models, we remove one dimension from the problem completely, which enormously reduces the computational demands of any simulations.

It is telling that, having studied this variational ansatz for $\chi(z)$, Wilson *et al.* returned to consider quasi-2D systems in subsequent publications.

A.2 Dipole-Dipole Potential

Here, we evaluate the dipole interaction potential as it appears in the GPE (equation 1.14) and elsewhere. The term we want to evaluate is

$$\int d\mathbf{x}' \ \psi^*(\mathbf{x}')V_d(\mathbf{x}-\mathbf{x}')\psi(\mathbf{x}') \tag{A.5}$$

Since we are in quasi-2D, we can also integrate out the z direction to remove the z dependence from the problem

$$\begin{aligned}
&\int dz \ \chi^*(z)\left\{\int d\mathbf{x}' \ \psi^*(\mathbf{x}')V_d(\mathbf{x}-\mathbf{x}')\psi(\mathbf{x}')\right\}\chi(z) \\
&= \int dz \ \chi^*(z)\left\{\int d\boldsymbol{\rho}' \int dz' \ \psi^*(\boldsymbol{\rho}')\chi^*(z)V_d(\mathbf{x}-\mathbf{x}')\psi(\boldsymbol{\rho}')\chi(z')\right\}\chi(z) \\
&= \int d\boldsymbol{\rho}' \ |\psi(\boldsymbol{\rho})|^2 \underbrace{\int dz \int dz' \ \chi^*(z)\chi^*(z')V_d(\mathbf{x}-\mathbf{x}')\chi(z')\chi(z)}_{V_d(\boldsymbol{\rho}-\boldsymbol{\rho}')}
\end{aligned} \tag{A.6}$$

To evaluate this integral, let us consider the interaction potential of identical dipole moments aligned along the z direction.

$$V_d(\mathbf{x}) = \frac{d^2}{\mathbf{x}^3}\left(1-3(\hat{\mathbf{x}}\cdot\hat{\mathbf{d}})^2\right) \tag{A.7}$$

The fourier transform of $V_d(\mathbf{x})$ is given by

$$\tilde{V}_d(\mathbf{k}) = g_{dd}\left(3\left(\frac{k_z}{k}\right)^2 - 1\right) \tag{A.8}$$

Now, for reasons that will be apparent in a moment, let us consider the following integral

$$\tilde{V}_d(\mathbf{k}_\rho) = \int dk_z \tilde{n}(k_z)^2 \tilde{V}_d(\mathbf{k}) \tag{A.9}$$

To calculate $\tilde{n}_z(k_z)$, recall that in the quasi-2D regime we assume the axial wavefunction takes the explicit form $\chi(z)$ given in equation 1.4. From this, we find

$$\tilde{n}_z(k_z) = \mathcal{F}(|\chi(z)|^2) = \exp\left(-\frac{1}{4}k_z^2 l_z^2\right) \tag{A.10}$$

so we can evaluate the integral A.9 to give

$$\begin{aligned}\tilde{V}_d(\mathbf{k}_\rho) &= g_{dd}\int dk_z\ e^{-\frac{1}{2}{k_z}^2{l_z}^2}\left(3\left(\frac{k_z}{k}\right)^2-1\right)\\ &= \frac{g_{dd}}{\sqrt{2\pi}l_z}F\left(\frac{\mathbf{k}_\rho l_z}{\sqrt{2}}\right)\end{aligned} \tag{A.11}$$

where

$$F(\mathbf{q}) = 2-3\sqrt{\pi}qe^{q^2}\mathrm{erfc}(\mathbf{q}) \tag{A.12}$$

We are interested in this integral because it is the Fourier transform of $V_d(\boldsymbol{\rho}-\boldsymbol{\rho}')$, the term that we were interested in equation A.6. (I will not prove that this is the case, but I refer the reader to Appendix A of [9].)

Seeing that we have acquired the Fourier transform of $V_d(\boldsymbol{\rho}-\boldsymbol{\rho}')$, we can now evaluate equation A.6 using the convolution theorem, to obtain

$$\begin{aligned}\int dz\ \chi^*(z)\left\{\int d\mathbf{x}'\ \psi^*(\mathbf{x}')V_d(\mathbf{x}-\mathbf{x}')\psi(\mathbf{x}')\right\}\chi(z) &= \int d\boldsymbol{\rho}'\ n(\boldsymbol{\rho}')V_d(\boldsymbol{\rho}-\boldsymbol{\rho}')\\ &= \mathcal{F}^{-1}\left(\tilde{n}(\mathbf{k}_\rho)\tilde{V}_d(\mathbf{k}_\rho)\right)\end{aligned} \tag{A.13}$$

where $n(\mathbf{k_\rho}) = \mathcal{F}(|\psi(\boldsymbol{\rho})|^2)$. This is the explicit form for the interaction integral that we desire. For brevity, we define $\Phi_D(\mathbf{x}) \coloneqq \mathcal{F}^{-1}\left(\tilde{n}(\mathbf{k}_\rho)\tilde{V}_d(\mathbf{k}_\rho)\right)$

A.3 Asymptotic Limit of the Complementary Error Function

When implementing dipolar interactions, we must consider the interaction potential in k-space. As discussed already, it takes the form

$$\tilde{V}_{\mathrm{d}}(\mathbf{k}_\rho) = g_{d,\mathrm{q2D}}F\left(\frac{\mathbf{k}_\rho l_z}{\sqrt{2}}\right) \qquad \text{where} \qquad F(\mathbf{q}) = 2-3\sqrt{\pi}q\exp^{q^2}\mathrm{erfc}(q) \tag{A.14}$$

MATLAB® handles $F(\mathbf{q})$ badly for large q since the exponential term grows very, very quickly while the complementary shrinks oppositely. MATLAB® tries to evaluate these two terms separately, and soon returns infinities. This can be resolved as follows.

For large q, the complementary error function is given by

$$\operatorname{erfc}(q) = \frac{e^{-x^2}}{q\sqrt{\pi}} \left(1 + \sum_{n=1}^{\infty} (-1)^n \frac{(2n-1)!!}{(2x^2)^n} \right) \tag{A.15}$$

where $(2n-1)!!$ is the double factorial: the product of all odd numbers up to $2n-1$.

Using this, $F(\mathbf{q})$ can be computed as

$$F(\mathbf{q}) = 2 - 3 \left(1 + \sum_{n=1}^{\infty} (-1)^n \frac{(2n-1)!!}{(2x^2)^n} \right) \tag{A.16}$$

Casting the complementary error function in this form resolves all the difficulties MATLAB® had in evaluating it.

A.4 Bogoliubov Quasiparticles in Dipolar Gases

In Section 1.5, we presented the results from diagonalising our system's Hamiltonian. In this appendix, we explicitly carry out this diagonalisation process. As found in that section, the Hamiltonian of a quasi-2D system in a plane wave basis is given in by

$$\hat{H} = \sum_{\mathbf{k}} \frac{\hbar^2 k^2}{2m} \hat{a}_{\mathbf{k}}^{\dagger} \hat{a}_{\mathbf{k}} + \frac{1}{2L^2} \sum_{\mathbf{k}_1, \mathbf{k}_2, \mathbf{q}} \tilde{V}(\mathbf{q}) \hat{a}_{\mathbf{k}_1+\mathbf{q}}^{\dagger} \hat{a}_{\mathbf{k}_2-\mathbf{q}}^{\dagger} \hat{a}_{\mathbf{k}_1} \hat{a}_{\mathbf{k}_2} \tag{A.17}$$

Recall that having restricted ourselves to an ultracold gas that is almost exclusively in the condensate, we have $N_0 \gg 1$, and thus

$$\hat{a}_0 |N_0, 0, 0, ...\rangle \approx \sqrt{N_0} |N_0, 0, 0, ...\rangle \qquad \hat{a}_0^{\dagger} |N_0, 0, 0, ...\rangle \approx \sqrt{N_0} |N_0, 0, 0, ...\rangle \tag{A.18}$$

In light of this, Bogoliubov suggested the approximation $\hat{a}_0,\ \hat{a}_0^{\dagger} \to \sqrt{N_0}$ [15].

By employing this approximation, the Hamiltonian separates into terms proportional to ${N_0}^2$, ${N_0}^{3/2}$, N_0, and so on. Since $N_0 \gg 1$, these get progressively smaller. We use this approach to simplify the Hamiltonian of equation A.17. Keeping only terms up to order N_0, the kinetic part can be written as

$$\hat{H}_{\text{kin}} = \frac{1}{2} \sum_{\mathbf{k} \neq 0} \epsilon_k^0 \left(\hat{a}_{\mathbf{k}}^{\dagger} \hat{a}_{\mathbf{k}} + \hat{a}_{-\mathbf{k}}^{\dagger} \hat{a}_{-\mathbf{k}} \right) \tag{A.19}$$

Meanwhile, the interaction part of the Hamiltonian becomes

$$\hat{H}_{\text{int}} \approx \frac{1}{2L^2}\Bigg[{N_0}^2\tilde{V}(\mathbf{0}) + 2N_0\sum_{\mathbf{k}\neq 0}\tilde{V}(\mathbf{0})\left(\hat{a}^\dagger_{\mathbf{k}}\hat{a}_{\mathbf{k}}\right) + N_0\sum_{\mathbf{k}\neq 0}\tilde{V}(\mathbf{k})\left(\hat{a}^\dagger_{\mathbf{k}}\hat{a}_{\mathbf{k}} + \hat{a}^\dagger_{-\mathbf{k}}\hat{a}_{-\mathbf{k}}\right) + N_0\sum_{\mathbf{k}\neq 0}\tilde{V}(\mathbf{k})\left(\hat{a}^\dagger_{\mathbf{k}}\hat{a}^\dagger_{-\mathbf{k}} + \hat{a}_{\mathbf{k}}\hat{a}_{-\mathbf{k}}\right)\Bigg] \tag{A.20}$$

We've kept only the terms of N_0^2 and N_0 (the $N_0^{3/2}$ terms vanish). The three sums are called the direct, exchange, and pairing interactions respectively.

It is worthwhile writing N_0 as

$$N_0 = N - \sum_{\mathbf{k}\neq 0}\hat{a}^\dagger_{\mathbf{k}}\hat{a}_{\mathbf{k}} \tag{A.21}$$

because N (the number of particles in our cell) is fixed. Substituting this into A.20 gives

$$\hat{H} = \frac{1}{2}nN\tilde{V}(\mathbf{0}) + \frac{1}{2}\sum_{\mathbf{k}\neq 0}\left[(\epsilon^0_k + n\tilde{V}(\mathbf{k}))\left(\hat{a}^\dagger_{\mathbf{k}}\hat{a}_{\mathbf{k}} + \hat{a}^\dagger_{-\mathbf{k}}\hat{a}_{-\mathbf{k}}\right) + n\tilde{V}(\mathbf{k})\left(\hat{a}^\dagger_{\mathbf{k}}\hat{a}^\dagger_{-\mathbf{k}} + \hat{a}_{\mathbf{k}}\hat{a}_{-\mathbf{k}}\right)\right] \tag{A.22}$$

We've neglected terms like $(\sum_{\mathbf{k}\neq 0}\hat{a}_{\mathbf{k}}\hat{a}^\dagger_{\mathbf{k}})^2$, which will be comparatively small. Also note that the direct interactions have been cancelled entirely by introducing A.21.

This Hamiltonian is a quadratic form in the creation and annihilation operators. We can therefore diagonalise the Hamiltonian by introducing the "quasiparticle" operators $\hat{\alpha}^\dagger_k$ and $\hat{\alpha}_k$, where

$$\begin{aligned}\hat{a}_{\mathbf{k}} &= u_k\hat{\alpha}_{\mathbf{k}} - v_k\hat{\alpha}^\dagger_{-\mathbf{k}}\\ \hat{a}^\dagger_{-\mathbf{k}} &= u_k\hat{\alpha}^\dagger_{-\mathbf{k}} - v_k\hat{\alpha}_{\mathbf{k}}\end{aligned} \quad\Longrightarrow\quad \begin{aligned}\hat{\alpha}_{\mathbf{k}} &= u_k\hat{a}_{\mathbf{k}} + v_k\hat{a}^\dagger_{-\mathbf{k}}\\ \hat{\alpha}^\dagger_{-\mathbf{k}} &= u_k\hat{a}^\dagger_{-\mathbf{k}} + v_k\hat{a}_{\mathbf{k}}\end{aligned} \tag{A.23}$$

where u_k and v_k are some real coefficients. This transformation is canonical provided the Bose commutation relations are satisfied,

$$[\hat{\alpha}^\dagger_{\mathbf{k}}, \hat{\alpha}_{\mathbf{k}'}] = \delta_{\mathbf{k}\mathbf{k}'} \Longrightarrow u_k^2 - v_k^2 = 1 \tag{A.24}$$

Directly substituting this into the Hamiltonian gives

$$\begin{aligned}\hat{H} = \frac{1}{2}nN\tilde{V}(\mathbf{0}) + \sum_{\mathbf{k}\neq 0}\Big((\epsilon_k^0 + n\tilde{V}(\mathbf{k}))v_k^2 - n\tilde{V}(\mathbf{k})u_k v_k\Big) \\ + \frac{1}{2}\sum_{\mathbf{k}\neq 0}\Big((\epsilon_k^0 + n\tilde{V}(\mathbf{k}))(u_k^2+v_k^2) - 2n\tilde{V}(\mathbf{k})u_k v_k\Big)\left[\hat{\alpha}_{\mathbf{k}}^\dagger\hat{\alpha}_{\mathbf{k}} + \hat{\alpha}_{-\mathbf{k}}^\dagger\hat{\alpha}_{-\mathbf{k}}\right] \\ + \frac{1}{2}\sum_{\mathbf{k}\neq 0}\Big(n\tilde{V}(\mathbf{k})(u_k^2+v_k^2) - 2(\epsilon_k^0 + n\tilde{V}(\mathbf{k}))u_k v_k\Big)\left[\hat{\alpha}_{\mathbf{k}}^\dagger\hat{\alpha}_{-\mathbf{k}}^\dagger + \hat{\alpha}_{\mathbf{k}}\hat{\alpha}_{-\mathbf{k}}\right]\end{aligned} \tag{A.25}$$

This is diagonal in $\hat{\alpha}_{\mathbf{k}}^\dagger\hat{\alpha}_{\mathbf{k}}$ provided we choose u_k and v_k to satisfy

$$n\tilde{V}(\mathbf{k})(u_k^2+v_k^2) - 2(\epsilon_k^0 + n\tilde{V}(\mathbf{k}))u_k v_k = 0 \tag{A.26}$$

We can incorporate $u_k^2 - v_k^2 = 1$ by writing $u_k = \cosh\theta_k$ and $v_k = \sinh\theta_k$, so it follows that

$$\tanh(2\theta_k) = \frac{n\tilde{V}(\mathbf{k})}{\epsilon_k^0 + n\tilde{V}(\mathbf{k})} \Longrightarrow \theta_k = \frac{1}{2}\tanh^{-1}\left(\frac{n\tilde{V}(\mathbf{k})}{\epsilon_k^0 + n\tilde{V}(\mathbf{k})}\right) \tag{A.27}$$

From this, we can easily calculate u_k and v_k. This choice of u_k and v_k gives the Hamiltonian

$$\hat{H} = \frac{1}{2}nN\tilde{V}(\mathbf{0}) + \frac{1}{2}\sum_{\mathbf{k}\neq 0}\Big(E_k - \epsilon_k^0 - n\tilde{V}(\mathbf{k})\Big) + \frac{1}{2}\sum_{\mathbf{k}\neq 0}E_k\left(\hat{\alpha}_{\mathbf{k}}^\dagger\hat{\alpha}_{\mathbf{k}} + \hat{\alpha}_{-\mathbf{k}}^\dagger\hat{\alpha}_{-\mathbf{k}}\right) \tag{A.28}$$

where we define

$$E_k = \sqrt{(\epsilon_k^0 + n\tilde{V}(\mathbf{k}))^2 - (n\tilde{V}(\mathbf{k}))^2} = \sqrt{\epsilon_k^0(\epsilon_k^0 + 2n\tilde{V}(\mathbf{k}))} \tag{A.29}$$

Now, this Hamiltonian is diagonal. Of course, we have neglected higher order terms so the quasiparticles do not truly diagonalise the full Hamiltonian. It is also worthwhile noting that the form of the Hamiltonian makes it apparent that E_k is the dispersion relation of the gas.

A Note on Conventions

There are multiple conventions as to how the quasiparticle operators are defined. How we defined them, in equation A.23, is by no means unique. I have chosen to be consistent

with [47], as opposed to the conventions used by [12, 48, 49]

What is more noteworthy, however, is a subtlety of a common method for solving for u_k and v_k. Some authors provide the following solution:

$$v_k^2 = u_k^2 - 1 = \frac{1}{2}\left(\frac{\epsilon_k^0 + n\tilde{V}(\mathbf{k})}{E_k} - 1\right) \tag{A.30}$$

However, this approach only works properly if u_k and v_k are positive. (The authors who use this approach are usually treating a situation with contact interactions only, in which case $n\tilde{V}(\mathbf{k}) = ng$, so this assumption is quite reasonable.) For a dipolar gas, it is possible for u_k and v_k to run negative while the gas remains stable. In this case, we must use the the solution involving θ_k.

A.5 An Alternative Approach; the Bogoliubov de Gennes Equations

Consider again the Gross-Pitaevskii Equation

$$i\hbar\frac{\partial}{\partial t}\psi(\mathbf{x},t) = \left(\hat{H}^{(1)} + \int d\mathbf{x}'\ \psi^*(\mathbf{x},t)V(\mathbf{x}-\mathbf{x}')\psi(\mathbf{x},t)\right)\psi(\mathbf{x},t)$$

In Section 1.5 we treated excitations of this system by considering quasiparticles, whose introduction diagonalised the Hamiltonian to first order. I claimed that this is equivalent to linearising small oscillations in the Gross-Pitaevskii Equation.

Here, I want to demonstrate this equivalence. The following linearisation procedure offers an intuitive way of considering the Bogoliubov approximation, and equips us with a few results I called on in this dissertation.

In the ultra-cold regime, the system is almost fully condensed, so $N_0/N \approx 1$. Therefore, we can make the approximation that the field operator can be separated into a large condensate fraction and a small fluctuation operator

$$\hat{\psi} \cong \psi_0 + \hat{\varphi} \tag{A.31}$$

where ψ_0 is normalised to N_0 and $\hat{\varphi}$ satisfies the bosonic commutation relations

$$\left[\hat{\varphi}(\mathbf{x}), \hat{\varphi}^\dagger(\mathbf{x}')\right] = \delta(\mathbf{x}-\mathbf{x}') \qquad \left[\hat{\varphi}(\mathbf{x}), \hat{\varphi}(\mathbf{x}')\right] = \left[\hat{\varphi}^\dagger(\mathbf{x}), \hat{\varphi}^\dagger(\mathbf{x}')\right] = 0 \tag{A.32}$$

This approximation can be used to rewrite the Hamiltonian. Unfortunately, this prescription means that particle number is no longer conserved, so we must introduce a grand canonical Hamiltonian $\hat{K} = \hat{H} - \mu\hat{N}$ with the chemical potential μ. The chemical potential acts as Lagrange multiplier that ensures that the number of particles is conserved.

We can express $\hat{K}$ perturbatively as $\hat{K} = K_0 + \hat{K}_1 + \hat{K}_2 + ...$ where $\hat{K}_i$ contains the terms of i^{th} order in the fluctuations $\hat{\varphi}(\mathbf{x})$. In this expansion, the zeroth order term is

$$K_0 = \int d\mathbf{x}\ \psi_0^*(\mathbf{x}) \left(\hat{H}^{(1)} - \mu\right) \psi_0(\mathbf{x}) + \frac{1}{2}\int\int d\mathbf{x}\ d\mathbf{x}'\ \psi_0^*(\mathbf{x})\psi_0^*(\mathbf{x}')V(\mathbf{x}-\mathbf{x}')\psi_0(\mathbf{x}')\psi_0(\mathbf{x}) \tag{A.33}$$

If we demand that $\psi_0(\mathbf{x})$ minimises K_0, we obtain

$$\mu\psi_0(\mathbf{x}) = \left(\hat{H}^{(1)}(\mathbf{x}) + \int d\mathbf{x}'\ \psi_0^*(\mathbf{x}')V(\mathbf{x}-\mathbf{x}')\psi_0(\mathbf{x}')\right)\psi_0(\mathbf{x}) \tag{A.34}$$

which is the Gross-Pitaevskii equation. We can easily see that this is satisfied by

$$\psi_0(\mathbf{x}) = \sqrt{n_0} \qquad \text{where} \qquad n_0 = \frac{N_0}{L^2} = \frac{\mu}{g + g_{dd}} \tag{A.35}$$

However, we are also interested in the higher order terms for our "Kamiltonian". The next non-zero term is the second order term

$$\begin{aligned}\hat{K}_2 = &\int d\mathbf{x}\ \hat{\varphi}^\dagger(\mathbf{x}) \left(\hat{H}^{(1)} - \mu\right)\hat{\varphi}(\mathbf{x}) + \frac{1}{2}\int\int d\mathbf{x}\ d\mathbf{x}'\ V(\mathbf{x}-\mathbf{x}') \\ &\times \Big\{\hat{\varphi}^\dagger(\mathbf{x})\hat{\varphi}^\dagger(\mathbf{x}')\psi_0(\mathbf{x}')\psi_0(\mathbf{x}) + \hat{\varphi}^\dagger(\mathbf{x})\psi_0^*(\mathbf{x}')\hat{\varphi}(\mathbf{x}')\psi_0(\mathbf{x}) + \hat{\varphi}^\dagger(\mathbf{x})\psi_0^*(\mathbf{x}')\psi_0(\mathbf{x}')\hat{\varphi}(\mathbf{x}) \\ &\quad + \psi_0^*(\mathbf{x})\hat{\varphi}^\dagger(\mathbf{x}')\psi_0(\mathbf{x}')\hat{\varphi}(\mathbf{x}) + \psi_0^*(\mathbf{x})\psi_0^*(\mathbf{x}')\hat{\varphi}(\mathbf{x}')\hat{\varphi}(\mathbf{x}) + \psi_0^*(\mathbf{x})\hat{\varphi}^\dagger(\mathbf{x}')\hat{\varphi}(\mathbf{x}')\psi_0(\mathbf{x})\Big\}\end{aligned} \tag{A.36}$$

If we now define $\mathcal{L} = \hat{H}^{(1)} - \mu + \int d\mathbf{x}'\ \psi_0^*(\mathbf{x}')V(\mathbf{x}-\mathbf{x}')\psi_0(\mathbf{x}')$, and assume that $V(\mathbf{x}-\mathbf{x}')$ is symmetric in $\mathbf{x}$ and $\mathbf{x}'$, this can be rewritten as

$$\begin{aligned}\hat{K}_2 = &\int d\mathbf{x}\ \hat{\varphi}^\dagger(\mathbf{x})\mathcal{L}\hat{\varphi}(\mathbf{x}) + \frac{1}{2}\int\int d\mathbf{x}\ d\mathbf{x}'\ V(\mathbf{x}-\mathbf{x}') \\ &\times \Big\{\hat{\varphi}^\dagger(\mathbf{x})\hat{\varphi}^\dagger(\mathbf{x}')\psi_0(\mathbf{x}')\psi_0(\mathbf{x}) + 2\hat{\varphi}^\dagger(\mathbf{x})\hat{\varphi}(\mathbf{x}')\psi_0^*(\mathbf{x}')\psi_0(\mathbf{x}) + \hat{\varphi}(\mathbf{x})\hat{\varphi}(\mathbf{x}')\psi_0^*(\mathbf{x}')\psi_0^*(\mathbf{x})\Big\}\end{aligned} \tag{A.37}$$

The dynamical equations for the fluctuation operators are

$$i\hbar\frac{\partial\hat{\varphi}}{\partial t} = [\hat{\varphi}, \hat{K}_2] \qquad \text{and} \qquad i\hbar\frac{\partial\hat{\varphi}^\dagger}{\partial t} = [\hat{\varphi}^\dagger, \hat{K}_2] \tag{A.38}$$

From equations and , it is straightforward to find the equations of motion

$$i\hbar\frac{\partial\hat{\varphi}(\mathbf{x})}{\partial t} = \left(\mathcal{L} + \hat{D}\right)\hat{\varphi}(\mathbf{x}) + \hat{C}\hat{\varphi}^\dagger(\mathbf{x}) \tag{A.39}$$

$$-i\hbar\frac{\partial\hat{\varphi}^\dagger(\mathbf{x})}{\partial t} = \hat{C}^*\hat{\varphi}(\mathbf{x}) + \left(\mathcal{L} + \hat{D}^*\right)\hat{\varphi}^\dagger(\mathbf{x}) \tag{A.40}$$

where we have defined the operators

$$\hat{C}f(\mathbf{x}) \coloneqq \int d\mathbf{x}'\psi_0(\mathbf{x}')V(\mathbf{x}-\mathbf{x}')f(\mathbf{x}')\psi_0(\mathbf{x}) \tag{A.41}$$

$$\hat{C}^*f(\mathbf{x}) \coloneqq \int d\mathbf{x}'\psi_0^*(\mathbf{x}')V(\mathbf{x}-\mathbf{x}')f(\mathbf{x}')\psi_0^*(\mathbf{x}) \tag{A.42}$$

$$\hat{D}f(\mathbf{x}) \coloneqq \int d\mathbf{x}'\psi_0^*(\mathbf{x}')V(\mathbf{x}-\mathbf{x}')f(\mathbf{x}')\psi_0(\mathbf{x}) \tag{A.43}$$

$$\hat{D}^*f(\mathbf{x}) \coloneqq \int d\mathbf{x}'\psi_0(\mathbf{x}')V(\mathbf{x}-\mathbf{x}')f(\mathbf{x}')\psi_0^*(\mathbf{x}) \tag{A.44}$$

We now assume $\hat{\varphi}(\mathbf{x})$ can be expanded as

$$\hat{\varphi}(\mathbf{x}) = \sum_{j\neq 0}\left[u_j(\mathbf{x})\hat{\alpha}_j e^{-i\omega_j t} - v_j^*(\mathbf{x})\hat{\alpha}_j^\dagger e^{i\omega_j t}\right] \tag{A.45}$$

where $\hat{\alpha}$ and $\hat{\alpha}^\dagger$ are some annihilation and creation operators that obey the Bosonic commutation relations, and $u_j(\mathbf{x})$ and $v_j(\mathbf{x})$ are some (as of yet unspecified) functions. Since we know that $\hat{\varphi}$ satisfies the bosonic commutation relations, it follows that $u_j(\mathbf{x})$ and $v_j(\mathbf{x})$ must satisfy

$$\int d\mathbf{x}\left(u_i^*(\mathbf{x})u_j(\mathbf{x}) - v_i^*(\mathbf{x})v_j(\mathbf{x})\right) = \delta_{ij} \tag{A.46}$$

Substituting equation A.45 into equations A.39 and A.40 yields the *Bogoliubov de*

Gennes equations:

$$\hbar\omega_j u_j(\mathbf{x}) = \left(\mathcal{L} + \hat{D}\right) u_j(\mathbf{x}) - \hat{C} v_j(\mathbf{x}) \tag{A.47}$$

$$-\hbar\omega_j v_j(\mathbf{x}) = \hat{C}^* u_j(\mathbf{x}) - \left(\mathcal{L} + \hat{D}^*\right) v_j(\mathbf{x}) \tag{A.48}$$

I have been deliberately suggestive in my use of the notation $u_j(\mathbf{x})$ and $v_j(\mathbf{x})$. In fact, the Bogoliubov de Gennes equations have the solutions

$$u_j(\mathbf{x}) = u_j \frac{e^{i\mathbf{k}_j\cdot\mathbf{x}}}{L} \tag{A.49}$$

$$v_j(\mathbf{x}) = v_j \frac{e^{i\mathbf{k}_j\cdot\mathbf{x}}}{L} \tag{A.50}$$

where u_j and v_j are the coefficients associated with the quasiparticle of wavevector $\mathbf{k}_j$.[1] Specifically,

$$\begin{aligned} u_j &= \cosh\left(\frac{1}{2}\tanh^{-1}\left(\frac{n\tilde{V}(\mathbf{k}_j)}{\epsilon_q^0 + n\tilde{V}(\mathbf{k}_j)}\right)\right) \\ v_j &= \sinh\left(\frac{1}{2}\tanh^{-1}\left(\frac{n\tilde{V}(\mathbf{k}_j)}{\epsilon_q^0 + n\tilde{V}(\mathbf{k}_j)}\right)\right) \end{aligned} \tag{A.51}$$

To prove that A.49 and A.50 give a solution to A.47, we proceed as follows. Firstly, note that we have

$$\begin{aligned} \mathcal{L}\frac{e^{i\mathbf{k}_j\cdot\mathbf{x}}}{L} &= \left(\hat{H}^{(1)} - \mu + \int d\mathbf{x}'\ \psi_0^*(\mathbf{x}')V(\mathbf{x}-\mathbf{x}')\psi_0(\mathbf{x}')\right)\frac{e^{i\mathbf{k}_j\cdot\mathbf{x}}}{L} \\ &= \left(\epsilon_q^0 - \mu\right)\frac{e^{i\mathbf{k}_j\cdot\mathbf{x}}}{L} + \frac{n_0 e^{i\mathbf{k}_j\cdot\mathbf{x}}}{L}\int d\mathbf{x}' V(\mathbf{x}-\mathbf{x}') \\ &= \left(\epsilon_q^0 - \mu\right)\frac{e^{i\mathbf{k}_j\cdot\mathbf{x}}}{L} + \frac{n_0 e^{i\mathbf{k}_j\cdot\mathbf{x}}}{L}\tilde{V}(\mathbf{k}=\mathbf{0}) \\ &= \left(\epsilon_q^0 - \mu + n_0(g+2g_{dd})\right)\frac{e^{i\mathbf{k}_j\cdot\mathbf{x}}}{L} \\ &= \epsilon_q^0\frac{e^{i\mathbf{k}_j\cdot\mathbf{x}}}{L} \end{aligned} \tag{A.52}$$

[1] In the previous section, we denoted these u and v according their corresponding wavevector. To simplify notation here, I will instead refer to them by using indices.

and

$$\begin{aligned}\hat{C}\frac{e^{i\mathbf{k}_j\cdot\mathbf{x}}}{L} &= \int d\mathbf{x}'\psi_0(\mathbf{x}')V(\mathbf{x}-\mathbf{x}')\frac{e^{i\mathbf{k}_j\cdot\mathbf{x}'}}{L}\psi_0(\mathbf{x}) \\ &= \frac{n_0}{L}\int d\mathbf{r}V(\mathbf{r})\frac{e^{i\mathbf{k}_j\cdot(\mathbf{x}+\mathbf{r})}}{L} \\ &= \frac{e^{i\mathbf{k}_j\cdot\mathbf{x}}}{L}n_0\tilde{V}(\mathbf{k}_j)\end{aligned} \tag{A.53}$$

and

$$\begin{aligned}\hat{D}\frac{e^{i\mathbf{k}_j\cdot\mathbf{x}}}{L} &= \int d\mathbf{x}'\psi_0^*(\mathbf{x}')V(\mathbf{x}-\mathbf{x}')\frac{e^{i\mathbf{k}_j\cdot\mathbf{x}'}}{L}\psi_0(\mathbf{x}) \\ &= \frac{n_0}{L}\int d\mathbf{r}V(\mathbf{r})\frac{e^{i\mathbf{k}_j\cdot(\mathbf{x}+\mathbf{r})}}{L} \\ &= \frac{e^{i\mathbf{k}_j\cdot\mathbf{x}}}{L}n_0\tilde{V}(\mathbf{k}_j)\end{aligned} \tag{A.54}$$

We can then evaluate the right hand side of A.47:

$$\begin{aligned}\left(\mathcal{L}+\hat{D}\right)u_j(\mathbf{x}) - \hat{C}v_j(\mathbf{x}) &= \left\{\left(\epsilon_q^0 + \frac{n_0}{L}\tilde{V}(\mathbf{k}_j)\right)u_j - \frac{n_0}{L}\tilde{V}(\mathbf{k}_j)v_j\right\}e^{i\mathbf{q}\cdot\mathbf{x}} \\ &= \left\{\epsilon_q^0 + n_0\tilde{V}(\mathbf{k}_j)(1-v_j/u_j)\right\}\frac{u_j}{L}e^{i\mathbf{q}\cdot\mathbf{x}}\end{aligned} \tag{A.55}$$

We can evaluate the ratio v_j/u_j using A.51 to show that

$$\begin{aligned}\frac{v_j}{u_j} &= \tanh\left\{\frac{1}{2}\tanh^{-1}\left(\frac{n_0\tilde{V}(\mathbf{k}_j)}{\epsilon_q^0 + n_0\tilde{V}(\mathbf{k}_j)}\right)\right\} \\ &= \frac{1}{n_0\tilde{V}(\mathbf{k}_j)}\left(\epsilon_q^0 + n_0\tilde{V}(\mathbf{k}_j) - \sqrt{(\epsilon_q^0 + n_0\tilde{V}(\mathbf{k}_j))^2 - (n_0\tilde{V}(\mathbf{k}_j))^2}\right)\end{aligned} \tag{A.56}$$

in which case we can rewrite A.55 as

$$\begin{aligned}
&\left(\mathcal{L}+\hat{D}\right)u_j(\mathbf{x})-\hat{C}v_j(\mathbf{x})\\
&=\left\{\epsilon_q^0+n_0\tilde{V}(\mathbf{k}_j)-\left(\epsilon_q^0+n_0\tilde{V}(\mathbf{k}_j)-\sqrt{(\epsilon_q^0+n_0\tilde{V}(\mathbf{k}_j))^2-(n_0\tilde{V}(\mathbf{k}_j))^2}\right)\right\}u_j(\mathbf{x})\\
&=\sqrt{(\epsilon_q^0+n_0\tilde{V}(\mathbf{k}_j))^2-(n_0\tilde{V}(\mathbf{k}_j))^2}u_j(\mathbf{x})\\
&=\hbar\omega_j u_j(\mathbf{x})
\end{aligned} \tag{A.57}$$

so equation A.47 is indeed satisfied. The proof to show that A.48 is satisfied is entirely analogous.

Single Quasiparticle Dynamics

In Subsection 2.3 I claimed that

$$\begin{aligned}
\psi(\mathbf{x},t)&=e^{-i\mu t/\hbar}\left(\psi_0(\mathbf{x})+\lambda\vartheta(\mathbf{x},t)\right)\\
&=e^{-i\mu t/\hbar}\left(\psi_0(\mathbf{x})+\frac{\lambda}{L}\left[u_q e^{i(\mathbf{k}_q\cdot\mathbf{x}-\omega_q t)}-v_q e^{-i(\mathbf{k}_q\cdot\mathbf{x}-\omega_q t)}\right]\right)
\end{aligned}$$

satisfies the time dependent GPE equation. Here, I will prove that this is the case. Firstly, we have

$$i\hbar\frac{\partial}{\partial t}\psi(\mathbf{x},t)=\mu\psi(\mathbf{x},t)+\hbar\omega_q\frac{\lambda}{L}\left[u_q e^{i(\mathbf{k}_q\cdot\mathbf{x}-\omega_q t)}+v_q e^{-i(\mathbf{k}_q\cdot\mathbf{x}-\omega_q t)}\right]e^{-i\mu t/\hbar} \tag{A.58}$$

The kinetic term gives

$$-\frac{\hbar^2\nabla^2}{2m}\psi(\mathbf{x},t)=\lambda\epsilon_q^0\vartheta(\mathbf{x},t) \tag{A.59}$$

and finally, the interaction term yields

$$\begin{aligned}
&\left(\int\psi^*(\mathbf{x}',t)V(\mathbf{x}-\mathbf{x}')\psi(\mathbf{x}',t)d\mathbf{x}'\right)\psi(\mathbf{x},t)\\
&\quad=\left(\int\psi_0^*(\mathbf{x}',t)V(\mathbf{x}-\mathbf{x}')\psi_0(\mathbf{x}',t)d\mathbf{x}'\right)\psi_0(\mathbf{x},t)\\
&\qquad+\lambda\left(\int\psi_0^*(\mathbf{x}',t)V(\mathbf{x}-\mathbf{x}')\psi_0(\mathbf{x}',t)d\mathbf{x}'\right)\vartheta(\mathbf{x},t)\\
&\qquad+\lambda\hat{D}\vartheta(\mathbf{x}',t)+\lambda\hat{C}\vartheta^*(\mathbf{x}',t)
\end{aligned} \tag{A.60}$$

The zeroth order terms amount to the GPE, which is satisfied. The first order terms are

$$\hbar\omega_q \left[u_q e^{i(\mathbf{k}_q\cdot\mathbf{x}-\omega_q t)} + v_q e^{-i(\mathbf{k}_q\cdot\mathbf{x}-\omega_q t)}\right] = \mathcal{L}\vartheta(\mathbf{x},t) + \hat{D}\vartheta(\mathbf{x},t) + \hat{C}\vartheta^*(\mathbf{x},t) \tag{A.61}$$

Equating coefficients of $e^{\pm i\omega_q t}$ gives

$$\begin{aligned} \hbar\omega_q u_q e^{i\mathbf{k}_q\cdot\mathbf{x}} &= \left(\mathcal{L}+\hat{D}\right) u_q e^{i\mathbf{k}_q\cdot\mathbf{x}} - \hat{C} v_q e^{i\mathbf{k}_q\cdot\mathbf{x}} \\ -\hbar\omega_q v_q e^{i\mathbf{k}_q\cdot\mathbf{x}} &= \hat{C}^* v_q e^{i\mathbf{k}_q\cdot\mathbf{x}} - \left(\mathcal{L}+\hat{D}^*\right) u_q e^{i\mathbf{k}_q\cdot\mathbf{x}} \end{aligned} \tag{A.62}$$

Recognising these as the Bogoliubov de Gennes equations, we know these are satisfied for $u_q e^{i\mathbf{k}_q\cdot\mathbf{x}}$ and $v_q e^{i\mathbf{k}_q\cdot\mathbf{x}}$, as shown the previous Appendix. Therefore the proof is done: to first order, our "single quasiparticle" evolves as claimed in equation 2.19.

A.6 Calculating Density Fluctuations in MATLAB®

I spent a lot of time working out how to properly calculate the density fluctuation in MATLAB® of a quasi-2D gas. I include here an outline of what I found.

Firstly, consider the one dimensional Fourier transform. To implement the one-dimensional Fourier transform we use the MATLAB® commands `fft`, `fftshift` and `ifftshift`, which give

$$\begin{aligned} g[m] &= \texttt{ifftshift}(\texttt{fft}(\texttt{fftshift}(f[j]))) \\ &= \sum_{j=1}^{N} f[j] exp[-2\pi i(j-N/2-1)(m-N/2-1)/N] \end{aligned} \tag{A.63}$$

Note j and m are discrete indices, and $f[j]$ and $g[m]$ are $N\times 1$ vectors. The continuous transform we are trying to calculate is

$$g(k) = \int f(x) e^{-ikx}\, dx \tag{A.64}$$

(Note that we use the non-unitary transform to remain consistent with the Fourier

transform used in equation 3.16). If we discretise x and k as

$$x_j = (-N/2, -N/2+1, ..., N/2-1)\Delta x \tag{A.65}$$

$$k_j = (-N/2, -N/2+1, ..., N/2-1)\frac{2\pi}{N\Delta x} \tag{A.66}$$

we can rewrite the Fourier transform approximately as

$$\begin{aligned} g(k_m) &= \Delta x \sum_{j=1}^{N} f(x_j) e^{-ik_l x_j} \\ \implies g[m] &= \Delta x \sum_{j=1}^{N} f[j] \exp[-2\pi i (j - N/2 - 1)(m - N/2 - 1)/N] \\ &= \Delta x \ \texttt{ifftshift}(\texttt{fft}(\texttt{fftshift}(f[j])) \end{aligned} \tag{A.67}$$

Now, let's turn to the problem at hand: calculating density fluctuations. The density fluctuations are given by

$$S(k) = \frac{\langle |\delta n_k|^2 \rangle}{\mathcal{N}} \tag{A.68}$$

where $\mathcal{N}$ is the total number of particles (written here in script to avoid confusion with the grid size) and

$$\begin{aligned} \delta n_k &= \mathcal{F}\left(n(\mathbf{x}) - \overline{n}\right) \\ &= \int \left(|\psi(\mathbf{x})|^2 - \overline{|\psi(\mathbf{x})|^2} \right) e^{-i\mathbf{k}\cdot\mathbf{x}} d\mathbf{x} \\ &= \int\int \left(|\psi(x,y)|^2 - \overline{|\psi(x,y)|^2} \right) e^{-ik_x x} e^{-ik_y y} \ dx \ dy \end{aligned} \tag{A.69}$$

Calculating the two-dimensional Fourier transform involves no more than successive one-dimensional Fourier transforms in the x and y directions, and can be implemented via the command `fft2`. Consider $N \times N$ position and momentum grids constructed analogously to equations A.65 and A.66. Then we can calculate the transform as

$$\begin{aligned} g(k,q) &= \int\int f(x,y) e^{ik_x x} e^{ik_y y} \ dx \ dy \\ \implies g[m,n] &= (\Delta x)^2 \texttt{ifftshift}(\texttt{fft2}(\texttt{fftshift}(f[j,l])) \end{aligned} \tag{A.70}$$

Therefore the density fluctuations are calculated by

$$S[m,n] = \frac{(\Delta x)^4}{\mathcal{N}} \left\langle \left| \texttt{ifftshift}\left(\texttt{fft2}\left(\texttt{fftshift}\left(|\psi[j,l]|^2 - \overline{|\psi[j,l]|^2}\right)\right)\right)\right|^2 \right\rangle \quad \text{(A.71)}$$